

**AN ANALYSIS OF A NARROW-BAND  
FREQUENCY MODULATION  
INSTRUMENTATION PROBLEM**

---

**CLIFFORD A. SKINNER, JR.**











AN ANALYSIS OF A NARROW-BAND  
FREQUENCY MODULATION INSTRUMENTATION PROBLEM

\* \* \* \* \*

Clifford A. Skinner, Jr.

Released for general issue  
Cubic Corp. letter dtd 6/27/57





AN ANALYSIS OF A NARROW-BAND  
FREQUENCY MODULATION INSTRUMENTATION PROBLEM

by

Clifford A. Skinner, Jr.  
Lieutenant, United States Navy

Submitted in partial fulfillment of  
the requirements for the degree of

MASTER OF SCIENCE  
IN  
ENGINEERING ELECTRONICS

United States Naval Postgraduate School  
Monterey, California

1 9 5 7

Thesis  
S55

AN ANALYSIS OF A NARROW-BAND  
FREQUENCY MODULATION INSTRUMENTATION PROBLEM

by

Clifford A. Skinner, Jr.

This work is accepted as fulfilling  
the thesis requirements for the degree of

MASTER OF SCIENCE  
IN  
ENGINEERING ELECTRONICS

from the  
United States Naval Postgraduate School



## ABSTRACT

An approximate theoretical analysis is made of a phase discriminator to be used as a synchronous detector of a very narrow-band FM wave in noise. Experimental work is reported which indicates the superiority of this method of detection over a conventional FM discriminator.

A comparison is made of the effect upon limiter operating point of two different methods of automatic gain control. A simple diode detector is shown to be superior to a "carrier-only" method when the carrier-to-noise ratio varies over a large range.

The writer wishes to acknowledge the helpful assistance of the Study Group at Cubic Corporation and, in particular, that provided by Mr. Arthur E. Noyes and Mr. Homer A. Lasitter. The continued assistance and encouragement of Professors C. F. Klamm, Jr. and P. E. Cooper of the U. S. Naval Postgraduate School is sincerely appreciated. The informal preparatory course which they conducted during the Fall Term constituted an indispensable background for this investigation.



## TABLE OF CONTENTS

Section	Title	Page
1.	Introduction	1
2.	Characteristics of Random Noise	4
3.	Effect of a Linear Device Upon Random Noise	9
4.	Effect of a Non-Linear Device Upon Random Noise	10
5.	Analysis of a Phase Discriminator	12
6.	Comparison of Theoretical and Experimental Results for the Phase Discriminator	20
7.	Automatic Gain Control	29
8.	Conclusions	45
9.	Recommendations for Further Work	47
	Appendix A	49
	Appendix B	52
	Appendix C	55
	Bibliography	57





# LIST OF ILLUSTRATIONS

Figure		Page
1-1	Block Diagram of Proposed Transponder	3
5-1	Sketch of Proposed Phase Discriminator	12
6-1	Conversion of Frequency Discriminator to Phase Discriminator	20
6-2	Block Diagram of Laboratory Set-up	21
6-3	Oscilloscope Presentations	23
6-4	Theoretical Performance of Phase Dis- criminator	25
6-5	Experimental Performance of Phase Dis- criminator	26
6-6	Comparative Results for Large Reference Voltage	27
6-7	Comparative Results, Smaller $\beta_1$	28
7-1	Limiter Input Circuit	30
7-2	Limiter Equivalent Input Circuit	30
7-3	Phasor Diagram, $\beta_1 = .02$	41
7-4	Phasor Diagram, $\beta_1 = .163$	42



# TABLE OF SYMBOLS AND ABBREVIATIONS

$A_{\text{subscript}}$	Amplifier gain at frequency indicated by subscript
AGC	Automatic gain control
$\propto$	Arbitrary constant
$\propto_{\text{subscript}}$	Abbreviated form for $E_s \sin[\psi(t_{\text{sub}})]$
B	Bandwidth in cycles per second
$\beta_{\text{subscript}}$	Modulation index at point indicated by subscript
$\delta(f)$	Dirac Delta Function
$E_A$	D.C. self-bias voltage
$E_{R,S}$	Amplitude of sinusoidal wave at point indicated by subscript
$e_{\text{subscript}}$	Instantaneous voltage at point indicated by subscript
f	Frequency; function of variables in parentheses
$f_{\text{subscript}}$	Frequency indicated by subscript. ( $f_0 = 30$ Mc; $f_1 = 100$ Kc in experimental work; $f_1 = 491$ Kc in theoretical work)
$\mathcal{F}[ ]$	Fourier transform of term in brackets
$F(ju)$	Fourier transform of a current vs. voltage characteristic expressed as a function of $(ju)$ where $u$ is a variable of subsequent integration
$2\delta$	3-db bandwidth of a bandpass filter
G	Grid
$G(f), G(\omega)$	Power spectral density
$H(f)$	Fourier transform of $\rho^2(\tau)$
I.F.	Intermediate frequency (30 Mc)
$I_x$	Crystal diode current
$I_{x.d.c.}$	D.C. component of $I_x$



$j$	$\sqrt{-1}$
$K, k,$	Arbitrary constants
$n(t)$	Noise voltage
$\phi^{\text{superscript}}$	Phase delay at frequency indicated by superscript
$\phi(\tau)$	Autocorrelation function in I.F.
$\phi_o(\tau)$	Autocorrelation function of output
$\psi(t)$	Modulating voltage
$\psi(t_1, t_2)$	Characteristic function
$P_t$	Mean-square voltage in I.F. amplifier
$\rho(\tau)$	Normalized autocorrelation function
$R$	$E_R/E_s$
$R_x$	Grid-cathode internal resistance
$S_1$	Carrier-to-noise ratio (in I.F. amplifier)
$S_1'$	Carrier-to-noise ratio after bandwidth reduction
$S_2$	Signal-to-noise ratio (post-detection)
$\sigma^2$	Mean-square noise voltage
$T(S_1)$	Abbreviated expression for a longer function of $S_1$
$\tau$	Time interval between $t_1$ and $t_2$
$W_{\text{subscript}}$	Probability distribution indicated by subscript
$x(t), y(t)$	Quadrature components of $n(t)$ . Values at specific times indicated by subscripts, e.g., $x(t_2) = x_2$
$\mathbb{Z}$	Dummy variable used for convenience
$\text{~~~~~}$	Time average of the quantity beneath wavy line
$\text{—————}$	Ensemble average of the quantity beneath solid line



ave.

Time or ensemble average of the term following



Approaches

D

Equal by definition





## 1. Introduction.

Cubic Corporation of San Diego, California, produces a Distance Measuring Equipment of the phase comparison type. When used for missile tracking the ground station transmits a carrier in the 200-400 Mc frequency range, frequency modulated by five lower frequencies. These frequencies are selected to permit unambiguous range determination out to one-half the wavelength of the lowest frequency. The missile being tracked carries a transponder which receives the signal from the ground, extracts the modulating frequencies and remodulates a carrier of a different frequency which is transmitted to the ground.

The accuracy of the entire system depends upon the phase shift experienced by the modulating wave as it passes through the transponder. A constant phase shift can be calibrated out by simply adjusting the range indicating servo at the ground station to a known range. Thus it is desirable to use an I.F. strip which exhibits a linear phase shift vs. frequency characteristic over a large range of input signal level. Van Voorhis has shown that synchronously-tuned stages are very tolerant to changes in tube capacity and their simplicity makes them desirable for this purpose (23).<sup>\*</sup> Cubic's I.F. strips have six synchronously-tuned stages. The Q of plate tank circuits is deliberately made low (about 5.25) to decrease the steepness of the phase characteristic at midband and improve linearity at higher

<sup>\*</sup> Numbers in parentheses refer to bibliography.



and lower frequencies; stated differently, the overall bandwidth of the I.F. strip is established by adjusting Q.

To insure operation within the relatively linear portion of the phase vs. frequency characteristic, Cubic has considered it necessary to decrease the effective modulation index ( $\beta_{I.F.}$ ) to a value sufficiently small that only the first-order side-bands of the highest modulating frequency are significant. The method of negative feedback developed by Chaffee (4, 7, 8) is used to reduce  $\beta_{I.F.}$  to approximately .02. The feedback voltage is actually a portion of the re-transmitted signal which is offset from the incoming signal by the I.F. frequency of 30 Mc.

The I.F. strip is followed by a limiter and Foster-Seeley discriminator. It has been Cubic's experience that the modulating signal power out of the discriminator must exceed noise power by about 10 db to permit accurate determination of range. Since this deterioration of signal-to-noise ratio marks the limit of useful range, consideration was given to methods of improving performance. Several suggested changes were collected in an unpublished proposal submitted to the U. S. Air Force. Fig. (1-1) is a block diagram of the proposed transponder. It is the purpose of this paper to investigate certain of these suggested changes.



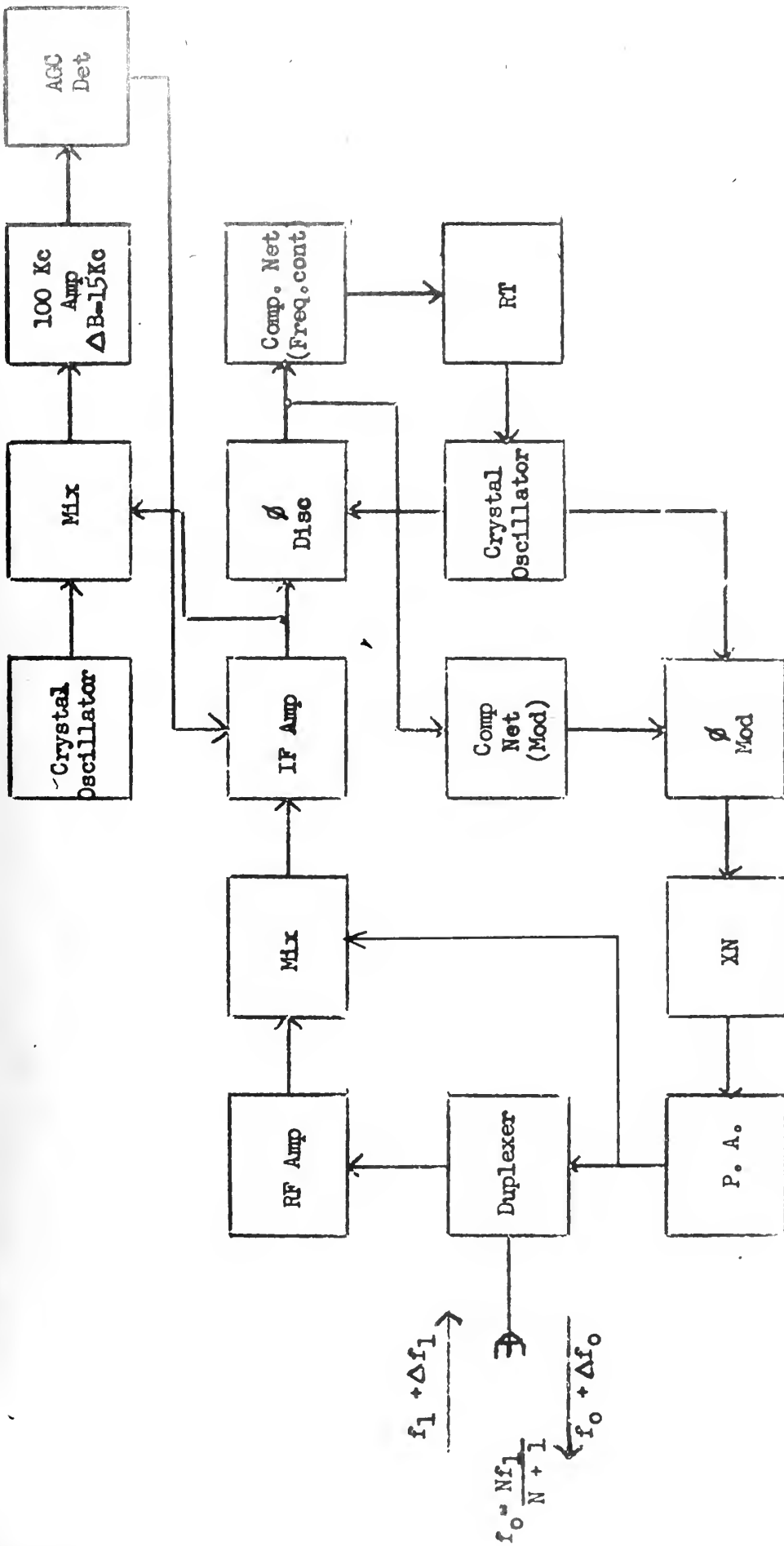


Fig. (1-1) -- DOPPLER TYPE TRANSPONDER - CORRELATION DETECTOR - COHERENT CARRIER



## 2. Characteristics of Random Noise.

In recent years much has been written about the detection of signals in noise. A rigorous treatment of any such problem requires the use of probability, since typical receiver noise is a random process.

This process cannot be written as an explicit function of time, for even if its exact values over a long interval of time are known, future values cannot be predicted precisely. It is possible, however, to determine the probability that the process will assume a certain value at any instant. This determination may be made from the observed values taken on by the process over an infinitely long interval of time, or by calculations when the characteristics of the primary source are known. Following the notation of Lawson and Uhlenbeck (16), this probability will be called the first probability distribution and is written  $W_1(y, t)$ , where  $y(t)$  is the random process and  $t$  is any instant of time. The assumption is made that the process is stationary, that is, any initial transients have decayed to negligibly small values and the process will display the same statistical properties over any (equal) long intervals of time.

In a similar way an expression may be written for the probability that  $y(t)$  will lie in the range  $y_1 + \Delta y_1$  at time  $t_1$  and in the range  $y_2 + \Delta y_2$  at a later time  $t_2$ . This probability is called the second probability distribution and is written  $W_2(y_1, t_1; y_2, t_2)$  or more simply





$W_2(y_1, y_2; \tau)$ , where  $\tau = t_2 - t_1$ . Third and higher order probability distributions may be written, each describing the process in more detail. As Lawson and Uhlenbeck have pointed out on p. 35 of their book, this series of distributions completely defines the process.

A convenient concept in this work is that of ensemble and time averages (16). If the random process  $y(t)$  is recorded for a very long interval of time and then this recording cut into a large number ( $N$ ) of intervals of length  $\Theta$ , this ensemble of recordings may be considered the simultaneous outputs of  $N$  identical receivers. Now the average value of a function of  $y$  at a time  $t$  may be written

$$\overline{f(y)} = \int_{-\infty}^{\infty} dy f(y) W_1(y, t) \quad (2-1)$$

where the bar indicates an ensemble average. This average is, in general, a function of  $t$ . If the average over time is performed the result is expressed as  $\overline{f}$ , where the wavy line indicates a time average. If the averaging is carried out in the reverse order the result is expressed as  $\overline{f}$ . The two methods yield the same answer since the infinite time average of  $y(t)$  is obtained in either case. If the process is stationary,  $\overline{f(y)} = \overline{f(y)}$ , since  $\overline{f(y)}$  is independent of time and  $\overline{f(y)}$  is the same for every member of the ensemble.



Of special interest is the average value of  $y(t)y(t+\tau)$ . Denoting this average by  $\phi(\tau)$ , it may be written

$$\phi(\tau) = \overline{y(t)y(t+\tau)} = \overline{y_1 y_2}.$$

$\phi(\tau)$  is called the autocorrelation function of  $y(t)$ , and for a stationary process becomes

$$\begin{aligned} \phi(\tau) &= \int \int_{-\infty}^{\infty} dy_1 dy_2 y_1 y_2 W_2(y_1, y_2; \tau) \\ &= \lim_{\Theta \rightarrow \infty} \frac{1}{\Theta} \int_{-\Theta/2}^{\Theta/2} y(t)y(t+\tau) dt. \end{aligned} \quad (2-2)$$

It is seen that  $\phi(0) =$  mean square value of  $y(t)$ . If the average value of  $y$  is zero,  $\phi(0) \stackrel{D}{=} \sigma^2 =$  variance.

The importance of the autocorrelation function lies in the fact that  $\phi(\tau)$  and  $G(\omega)$ , the power spectral density, are the Fourier transforms of each other (24):

$$\phi(\tau) = \frac{1}{2\pi} \int_{-\infty}^{\infty} \overline{G(\omega)} e^{j\omega\tau} d\omega = \int_0^{\infty} \overline{G(f)} \cos 2\pi f\tau df,$$

$$\overline{G(\omega)} = \int_{-\infty}^{\infty} \phi(\tau) e^{-j\omega\tau} d\tau, \quad (2-3)$$

$$\overline{G(f)} = 4 \int_0^{\infty} \phi(\tau) \cos 2\pi f\tau d\tau.$$



In a large class of problems, the probability density functions for random noise voltages are relatively simple mathematical expressions. Lawson and Uhlenbeck (16) and Rice (19) are among those who have shown that typical receiver noise sources, such as shot effect, thermal noise, induced grid noise, etc., are characterized by a normal or Gaussian probability density function of the form

$$W_1(y, t) = \frac{1}{\sqrt{2\pi}\sigma^2} e^{-\frac{y^2}{2\sigma^2}}. \quad (2-4)$$

Chapter 4 of Lawson and Uhlenbeck's book and Part II of Rice's paper contain extensive references to the literature. Knudtson (15) has published experimental verification for a variety of primary sources by measuring the autocorrelation function using sampling techniques and then computing the power spectrum with an electronic differential analyzer.

Two different representations of the random noise voltage will be found useful here. In the first form the voltage is called  $n(t)$ , with a first probability distribution

$$W_1(n) = \frac{1}{\sqrt{2\pi}\sigma^2} e^{-\frac{n^2}{2\sigma^2}}. \quad (2-5)$$

In the second form the noise voltage is developed in a Fourier series occupying a narrow band around the I.F. frequency  $f_0$ , such that (16)

$$n(t) = x(t) \cos 2\pi f_0 t + y(t) \sin 2\pi f_0 t, \quad (2-6)$$



where

$$x(t) = \sum_{k=-\infty}^{\infty} (a_k \cos 2\pi f_k t + b_k \sin 2\pi f_k t),$$

$$y(t) = \sum_{k=-\infty}^{\infty} (-a_k \sin 2\pi f_k t + b_k \cos 2\pi f_k t),$$

and  $f_k$  is measured from  $f_0$ . The  $a_k$  and  $b_k$  are independent random variables and  $x$  and  $y$  are orthogonal functions such that

$$\overline{x^2(t)} = \overline{y^2(t)} = \sigma^2,$$

$$\overline{x(t) y(t+\tau)} \equiv 0 \quad \text{for all } \tau, \quad (2-7)$$

$$\overline{x(t) x(t+\tau)} = \overline{y(t) y(t+\tau)} = \phi(\tau).$$

Hence,

$$W_1(x, y) = \frac{1}{2\pi\sigma^2} e^{-\frac{x^2 + y^2}{2\sigma^2}} \quad (2-8)$$

and

$$W_2(x_1, y_1; x_2, y_2; \tau) = \frac{1}{(2\pi\sigma^2)^2(1-\rho^2)} \exp\left(-\frac{1}{2\sigma^2(1-\rho^2)} \cdot \left\{x_1^2 + y_1^2 + x_2^2 + y_2^2 - 2\rho[x_1 x_2 + y_1 y_2]\right\}\right), \quad (2-9)$$

where

$$\rho = \rho(\tau) = \frac{\phi(\tau)}{\phi(0)} = \frac{\phi(\tau)}{\sigma^2}.$$





### 3. Effect of a Linear Device Upon Random Noise.

It is seen from Eq. (2-3) above that if  $G(\omega)$  is a constant for all values of  $\omega$ , then

$$\phi(\tau) = \begin{cases} \sigma^2 & , \quad \tau = 0 \\ 0 & , \quad \text{elsewhere} \end{cases}$$

and the correlation between successive values of  $y$  is zero. This limiting case is called the "purely random process" (11) and the associated spectrum a "white spectrum". When such noise is modified by a linear device so that the output spectrum has the shape of the power frequency response of the device, the output voltage is still Gaussian (16) but the autocorrelation function is no longer discontinuous.



#### 4. Effect of Non-Linear Devices Upon Random Noise.

Lawson and Uhlenbeck (16), Rice (19), Middleton (17, 18) and many others have published results of investigations of several types of non-linear devices under a variety of signal and noise conditions.

There are two generally accepted methods available for the study of the output of non-linear devices. In both of them the output power spectrum, at least in the range of interest, is determined. The first method, called by Rice the "direct method" and attributed by him to W. R. Bennett, F. C. Williams, J. R. Ragazzini and others, is based upon the known theory of modulation in non-linear devices. In this method a typical modulation product is computed and the output power spectrum then obtained by summing all such products.

The second method, attributed (19) to D. O. North, J. H. Van Vleck and D. Middleton, consists of first finding the autocorrelation function of the output, then taking the Fourier transform to give the power spectrum of the output. In this method use is frequently made of the characteristic function to more simply evaluate the autocorrelation function. The characteristic function is widely used by Lawson and Uhlenbeck throughout their book. Rice also uses the characteristic function approach in many cases because of its ready application to many devices expressible by the integral form



$$I = \int_C F(ju) e^{jVu} du, \quad (4-1)$$

where  $F(ju)$  is the Fourier transform of the I vs. V. characteristic of the device.

In many problems one of the methods may prove simpler mathematically than the other.



## 5. Analysis of a Phase Discriminator.

One of the changes suggested by Cubic is to replace the frequency discriminator with a phase discriminator which will be provided with a locally generated reference voltage in phase quadrature with the I.F. carrier wave. Cubic intends to supply this reference voltage by using an adaptation of the "active filter" designed by Jensen and McGeogh (14) to filter a portion of the I.F. signal which will then be shifted in phase by  $90^\circ$ . In this paper it will be assumed that the reference voltage is available.

A sketch of the proposed phase discriminator is shown below in Fig. (5-1).

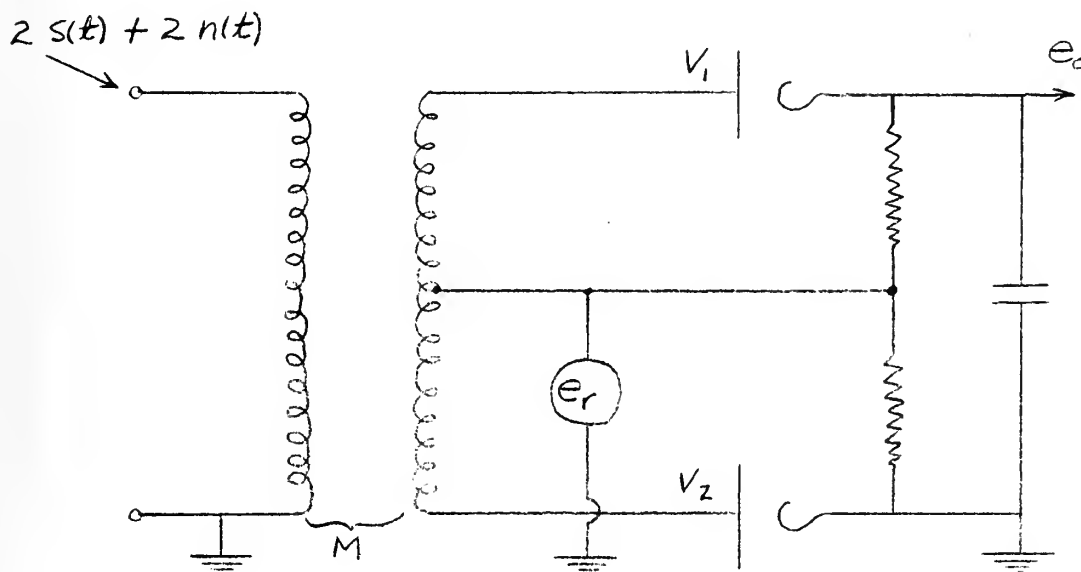


Fig. (5-1)





The voltages applied between the plates of V-1 and V-2, respectively, and R.F. ground are

$$e_1 = E_R \cos \omega_0 t + E_S \sin[\omega_0 t + \psi(t)] + n(t)$$

$$e_2 = E_R \cos \omega_0 t - E_S \sin[\omega_0 t + \psi(t)] - n(t)$$

or, since  $\psi$  is small,

$$e_1 = (E_R + E_S \sin \psi + x) \cos \omega_0 t + (E_S + y) \sin \omega_0 t \quad (5-1)$$

$$e_2 = (E_R - E_S \sin \psi - x) \cos \omega_0 t - (E_S + y) \sin \omega_0 t,$$

where  $n(t)$  has been expressed as in Eq. (2-6).

Considering the two diodes to be ideal linear rectifiers, the output voltage will be a high frequency wave with an envelope given by

$$e_o = \sqrt{(E_R + E_S \sin \psi + x)^2 + (E_S + y)^2} - \sqrt{(E_R - E_S \sin \psi - x)^2 + (E_S + y)^2}. \quad (5-2)$$

Expanding the expressions under the radicals and subtracting

$$\begin{aligned} e_o = & 2E_S \sin \psi + 2x + \frac{(E_S + y)^2}{2} \left[ \frac{1}{E_R + E_S \sin \psi + x} - \frac{1}{E_R - E_S \sin \psi - x} \right] \\ & - \frac{(E_S + y)^4}{8} \left[ \frac{1}{(E_R + E_S \sin \psi + x)^3} - \frac{1}{(E_R - E_S \sin \psi - x)^3} \right] \\ & + \frac{(E_S + y)^6}{16} \left[ \frac{1}{(E_R + E_S \sin \psi + x)^5} - \frac{1}{(E_R - E_S \sin \psi - x)^5} \right] + \dots \end{aligned}$$



Terms after the third are neglected since the condition will be imposed  $E_R \geq 5E_S$ . It is recognized that values of  $|X|$  and  $|y|$  equal to or greater than  $E_R$  will occur, but within the range of our interest the probability of occurrence will be very small. Hence

$$e_0 \doteq 2E_S \sin \psi + 2X + \frac{(E_S + y)^2}{2} \left[ \frac{1}{E_R + E_S \sin \psi + X} - \frac{1}{E_R - E_S \sin \psi - X} \right] \quad (5-3)$$

The binomial expansion is used again to expand the expression within square brackets.

$$\begin{aligned} & \left[ \frac{1}{E_R + E_S \sin \psi + X} - \frac{1}{E_R - E_S \sin \psi - X} \right] = \\ & = \left\{ \frac{1}{E_R} - \frac{E_S \sin \psi + X}{E_R^2} + \frac{(E_S \sin \psi + X)^2}{E_R^3} - + \dots \right\} \\ & - \left\{ \frac{1}{E_R} + \frac{E_S \sin \psi + X}{E_R^2} + \frac{(E_S \sin \psi + X)^2}{E_R^3} + \dots \right\} \\ & \doteq - \frac{2(E_S \sin \psi + X)}{E_R^2} \end{aligned}$$

where terms containing  $E_R$  to the fourth and higher powers in the denominator are neglected. Thus,

$$\begin{aligned} e_0 & \doteq 2E_S \sin \psi + 2X - \frac{(E_S + y)^2}{2} \cdot \frac{2(E_S \sin \psi + X)}{E_R^2} \\ & \doteq 2E_S \sin \psi + 2X - E_S \left[ \frac{E_S^2}{E_R^2} \sin \psi + \frac{E_S X}{E_R^2} + \frac{2E_S y \sin \psi}{E_R^2} \right. \\ & \quad \left. + \frac{2X y}{E_R^2} + \frac{y^2 \sin \psi}{E_R^2} + \frac{X y^2}{E_S E_R^2} \right] \end{aligned}$$



$$\begin{aligned}
&= 2 E_s \sin \psi \left[ 1 - \frac{1}{R^2} \right] + 2 x \left[ 1 - \frac{1}{R^2} \right] - \frac{2 x y}{E_s R^2} \\
&\quad - \frac{y^2 \sin \psi}{E_s R^2} - \frac{x y^2}{E_s^2 R^2} \quad (5-4)
\end{aligned}$$

where  $R = E_R/E_s$ .

Now denoting by subscripts the quantities at  $t_1$  and  $t_2$ , e.g.,  $x(t_1) = x_1$ ,  $y(t_2) = y_2$ , etc., and letting  $\alpha = E_s \sin \psi$ , the autocorrelation function of the output voltage may be written

$$\begin{aligned}
\phi_o(\tau) &= \overline{e_o(t) e_o(t+\tau)} = \text{ave.} \{ e_o(t_1) e_o(t_2) \} \\
&= \text{ave.} \left\{ 2\alpha_1 \left[ 1 - \frac{1}{R^2} \right] + 2x_1 \left[ 1 - \frac{1}{R^2} \right] - \frac{2y_1 \alpha_1}{E_s R^2} - \frac{2x_1 y_1}{E_s R^2} - \frac{y_1^2 \alpha_1}{E_s^2 R^2} - \frac{x_1 y_1^2}{E_s^2 R^2} \right\} \\
&\quad \cdot \left\{ 2\alpha_2 \left[ 1 - \frac{1}{R^2} \right] + 2x_2 \left[ 1 - \frac{1}{R^2} \right] - \frac{2y_2 \alpha_2}{E_s R^2} - \frac{2x_2 y_2}{E_s R^2} - \frac{y_2^2 \alpha_2}{E_s^2 R^2} - \frac{x_2 y_2^2}{E_s^2 R^2} \right\} \quad (5-5)
\end{aligned}$$

Twenty terms (of the 36) are zero because

$$\overline{\alpha_1} = \overline{\alpha_2} = \overline{x_1} = \overline{x_2} = \overline{y_1} = \overline{y_2} = 0.$$

Thus,

$$\begin{aligned}
\phi_o(\tau) &= 4 \overline{\alpha_1 \alpha_2} \left[ 1 - \frac{1}{R^2} \right]^2 - 2 \frac{\overline{\alpha_1 \alpha_2 y_1^2}}{E_s^2 R^2} \left[ 1 - \frac{1}{R^2} \right] + 4 \overline{x_1 x_2} \left[ 1 - \frac{1}{R^2} \right]^2 \\
&\quad - \frac{4 \overline{x_1 x_2 y_2}}{E_s R^2} \left[ 1 - \frac{1}{R^2} \right] - \frac{2 \overline{x_1 x_2 y_2^2}}{E_s^2 R^2} \left[ 1 - \frac{1}{R^2} \right] + \frac{4 \overline{y_1 y_2 \alpha_1 \alpha_2}}{E_s^2 R^4} \\
&\quad + \frac{2 \overline{y_1 \alpha_1 y_2^2 \alpha_2}}{E_s^3 R^4} - \frac{4 \overline{x_1 y_1 x_2}}{E_s R^2} \left[ 1 - \frac{1}{R^2} \right] + \frac{4 \overline{x_1 x_2 y_1 y_2}}{E_s^2 R^4}
\end{aligned}$$

(continued on following page)



$$\begin{aligned}
& + \frac{2 \overline{X_1 X_2 y_1 y_2}}{E_s^3 R^4} - \frac{2 \overline{y_1^2 \alpha_1 \alpha_2}}{E_s^2 R^2} \left[ 1 - \frac{1}{R^2} \right] + \frac{2 \overline{y_1^2 y_2 \alpha_1 \alpha_2}}{E_s^3 R^4} \\
& + \frac{\overline{y_1^2 y_2^2 \alpha_1 \alpha_2}}{E_s^4 R^4} - \frac{2 \overline{X_1 X_2 y_1^2}}{E_s^2 R^2} \left[ 1 - \frac{1}{R^2} \right] + \frac{2 \overline{X_1 X_2 y_1^2 y_2}}{E_s^3 R^4} \\
& + \frac{\overline{X_1 X_2 y_1^2 y_2^2}}{E_s^4 R^4} .
\end{aligned}$$

It is known that

$$\overline{X_1^2} = \overline{X_2^2} = \overline{y_1^2} = \overline{y_2^2} = \sigma^2.$$

Also,

$$\overline{X_1 X_2} = \overline{y_1 y_2} = \sigma^2 \rho(\tau).$$

The noise in the I.F. amplifier is taken to have a rectangular power spectrum of width B. Hence,

$$\phi(\tau) = \int_{-\infty}^{\infty} G_N(f) e^{j2\pi f\tau} df = \int_{-B/2}^{B/2} \frac{\sigma^2}{B} e^{j2\pi f\tau} df$$

$$= \frac{\sigma^2}{2\pi j\tau B} \left[ e^{j2\pi f\tau} \right]_{-B/2}^{B/2} = \sigma^2 \frac{\sin \pi \tau B}{\pi \tau B}$$

and

$$\rho(\tau) = \frac{\phi(\tau)}{\sigma^2} = \frac{\sin \pi \tau B}{\pi \tau B}.$$





Since  $x$  and  $y$  are independent, their joint probability distribution function may be written as a product, e.g.,

$$W_2(x_1, y_1; x_2, y_2; \tau) = \left\{ \frac{1}{2\pi\sigma^2\sqrt{1-\rho^2}} e^{-\frac{1}{2\sigma^2(1-\rho^2)}[x_1^2 + x_2^2 - 2\rho x_1 x_2]} \right\} \\ \cdot \left\{ \frac{1}{2\pi\sigma^2\sqrt{1-\rho^2}} e^{-\frac{1}{2\sigma^2(1-\rho^2)}[y_1^2 + y_2^2 - 2\rho y_1 y_2]} \right\}.$$

Thus the two terms containing  $\overline{x_1 x_2 y_2}$  and  $\overline{x_1 x_2 y_1}$  may be written respectively  $\overline{x_1 x_2} \cdot \overline{y_2}$  and  $\overline{x_1 x_2} \cdot \overline{y_1}$  and are both zero. By the same reasoning  $\overline{x_1 x_2 y_1^2} = \overline{x_1 x_2 y_2^2} = \sigma^4 \rho(\tau)$  and  $\overline{x_1 x_2 y_1 y_2} = \sigma^4 \rho^2(\tau)$ .

Calculation of the ensemble averages  $\overline{y_1 y_2^2}$ ,  $\overline{y_1^2 y_2}$ , and  $\overline{y_1^2 y_2^2}$  is most easily accomplished using the characteristic function method of Appendix (A). Thus

$$\psi(t_1, t_2) = e^{-\frac{\sigma^2}{2}[t_1^2 + 2\rho t_1 t_2 + t_2^2]}$$

and

$$\overline{y_1 y_2^2} = -j \left. \frac{\partial^3 \psi(t_1, t_2)}{\partial t_1 \partial^2 t_2} \right|_{t_1=0}^{t_2=0} \\ = -j \left[ \sigma^4 (t_1 + 2\rho t_2 + \rho^2 t_1) \psi - \sigma^6 (t_1 + \rho t_2)(t_2 + \rho t_1)(\rho t_1 + t_2) \psi \right]_{t_1=0}^{t_2=0} \\ = 0$$

Similarly,

$$\overline{y_1^2 y_2} = 0, \quad \overline{y_1^2 y_2^2} = \sigma^4(1 + 2\rho^2).$$



Thus,

$$\phi_0(\tau) = \overline{\alpha_1 \alpha_2} \left\{ 4 \left[ 1 - \frac{1}{R^2} \right]^2 - \frac{4\sigma^2}{E_s^2 R^2} \left[ 1 - \frac{1}{R^2} \right] + \frac{4\sigma^2 \rho}{E_s^2 R^4} + \frac{\sigma^4 (1+2\rho^2)}{E_s^4 R^4} \right\} \\ + 4\sigma^2 \rho \left[ 1 - \frac{1}{R^2} \right]^2 - \frac{4\sigma^4 \rho}{E_s^2 R^2} \left[ 1 - \frac{1}{R^2} \right] + \frac{4\sigma^4 \rho^2}{E_s^2 R^4} + \frac{\sigma^6 \rho (1+2\rho^2)}{E_s^4 R^4}. \quad (5-6)$$

Before calculating  $\overline{\alpha_1 \alpha_2}$  the assumption will be made that only one modulating frequency ( $f_1$ ) is present and that the effective modulation index is  $\beta_1$ . Using the approximation

$$\sin \psi \doteq \psi = \beta_1 \sin \omega_1 t$$

the calculation is made simpler and a direct comparison may be made with the experimental results of Section (6). Thus,

$$\overline{\alpha_1 \alpha_2} = E_s^2 \beta_1^2 \overline{\sin \omega_1 t \sin \omega_1 (t + \tau)} \\ = E_s^2 \beta_1^2 \cdot \frac{1}{2\pi} \int_0^{2\pi} \sin x \sin (x + \omega_1 \tau) dx \\ = \frac{E_s^2 \beta_1^2}{2\pi} \left\{ \cos \omega_1 \tau \int_0^{2\pi} \sin^2 x dx + \sin \omega_1 \tau \int_0^{2\pi} \sin x \cos x dx \right\} \\ = \frac{E_s^2 \beta_1^2}{2} \cos \omega_1 \tau$$

and

$$\phi_0(\tau) = \frac{E_s^2 \beta_1^2 \cos \omega_1 \tau}{2} \left\{ 4 \left[ 1 - \frac{1}{R^2} \right]^2 - \frac{4\sigma^2}{E_s^2 R^2} \left[ 1 - \frac{1}{R^2} \right] + \frac{4\sigma^2 \rho}{E_s^2 R^4} + \frac{\sigma^4 (1+2\rho^2)}{E_s^4 R^4} \right\} \\ + 4\sigma^2 \rho \left[ 1 - \frac{1}{R^2} \right]^2 - \frac{4\sigma^4 \rho}{E_s^2 R^2} \left[ 1 - \frac{1}{R^2} \right] + \frac{4\sigma^4 \rho^2}{E_s^2 R^4} + \frac{\sigma^6 \rho (1+2\rho^2)}{E_s^4 R^4}. \quad (5-7)$$



The power spectrum of the output is found by taking the Fourier transform of this expression. Using the results of Appendix (B), and writing the spectrum in positive frequencies only,

$$\begin{aligned}
 G_o(f) = & \left\{ 4 \left[ 1 - \frac{1}{R^2} \right]^2 - \frac{4\sigma^2}{E_s^2 R^2} \left[ 1 - \frac{1}{R^2} \right] + \frac{\sigma^4}{E_s^4 R^4} \right\} \cdot \frac{E_s^2 \beta_1^2}{2} \delta(f - f_1) \\
 & + \left( \frac{2\sigma^2}{E_s^2 R^4} \right) E_s^2 \beta_1^2 \cdot \begin{cases} 2/B, & 0 < f < \frac{B}{2} - f_1 \\ 1/B, & \frac{B}{2} - f_1 < f < \frac{B}{2} + f_1 \\ 0, & \text{elsewhere} \end{cases} \\
 & + \left( \frac{\sigma^4}{E_s^4 R^4} \right) \left( \frac{E_s^2 \beta_1^2}{B} \right) \cdot \begin{cases} 2 - \frac{2f_1}{B}, & 0 < f < f_1 \\ 2 - \frac{2f}{B}, & f_1 < f < B - f_1 \\ 1 - \frac{f - f_1}{B}, & B - f_1 < f < B + f_1 \\ 0, & \text{elsewhere} \end{cases} \\
 & + \left\{ 4\sigma^2 \left[ 1 - \frac{1}{R^2} \right] - \frac{4\sigma^2}{E_s^2 R^2} \left[ 1 - \frac{1}{R^2} \right] + \frac{\sigma^6}{E_s^4 R^4} \right\} \cdot \begin{cases} \frac{2}{B}, & 0 < f < \frac{B}{2} \\ 0, & \text{elsewhere} \end{cases} \\
 & + \frac{4\sigma^4}{E_s^2 R^4} \cdot \begin{cases} \frac{2}{B} \left[ 1 - \frac{f}{B} \right], & 0 < f < B \\ 0, & \text{elsewhere} \end{cases} \\
 & + \left( \frac{2\sigma^6}{E_s^4 R^4} \right) \left( \frac{2}{B^2} \right) \cdot \begin{cases} \left( \frac{3}{4} B - \frac{f^2}{B} \right), & 0 < f < \frac{B}{2} \\ \frac{9}{8} B - \frac{3}{2} f + \frac{f^2}{2B}, & \frac{B}{2} < f < \frac{3}{2} B \\ 0, & \text{elsewhere. (5-8)} \end{cases}
 \end{aligned}$$



## 6. Comparison of Theoretical and Experimental Results for the Phase Discriminator.

In the work at Cubic an accurate comparison was desired of the relative performance of the frequency discriminator in present use and the phase discriminator. Accordingly, laboratory tests were conducted using an actual transponder I.F. strip and frequency discriminator. The latter was converted to a phase discriminator by disconnecting the end of  $C_1$  marked S (see sketch below) from the primary of the transformer and feeding the reference voltage through  $C_1$ . The reference voltage entered through a shielded cable, the lead of  $C_1$  being the only unshielded path in both circuit configurations.

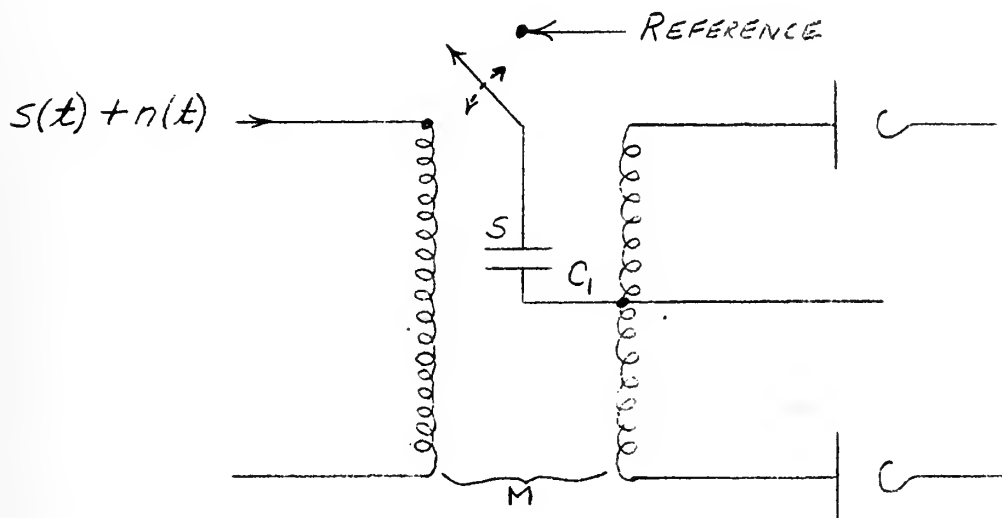


Fig. (6-1)

The complete laboratory set-up is shown in Fig. (6-2). The noise voltage  $n(t)$  was tube noise and thermal noise from the I.F. stages; carrier-to-noise (21) ratio ( $S_1$ ) was decreased by reducing the signal level.





# TEST SET-UP

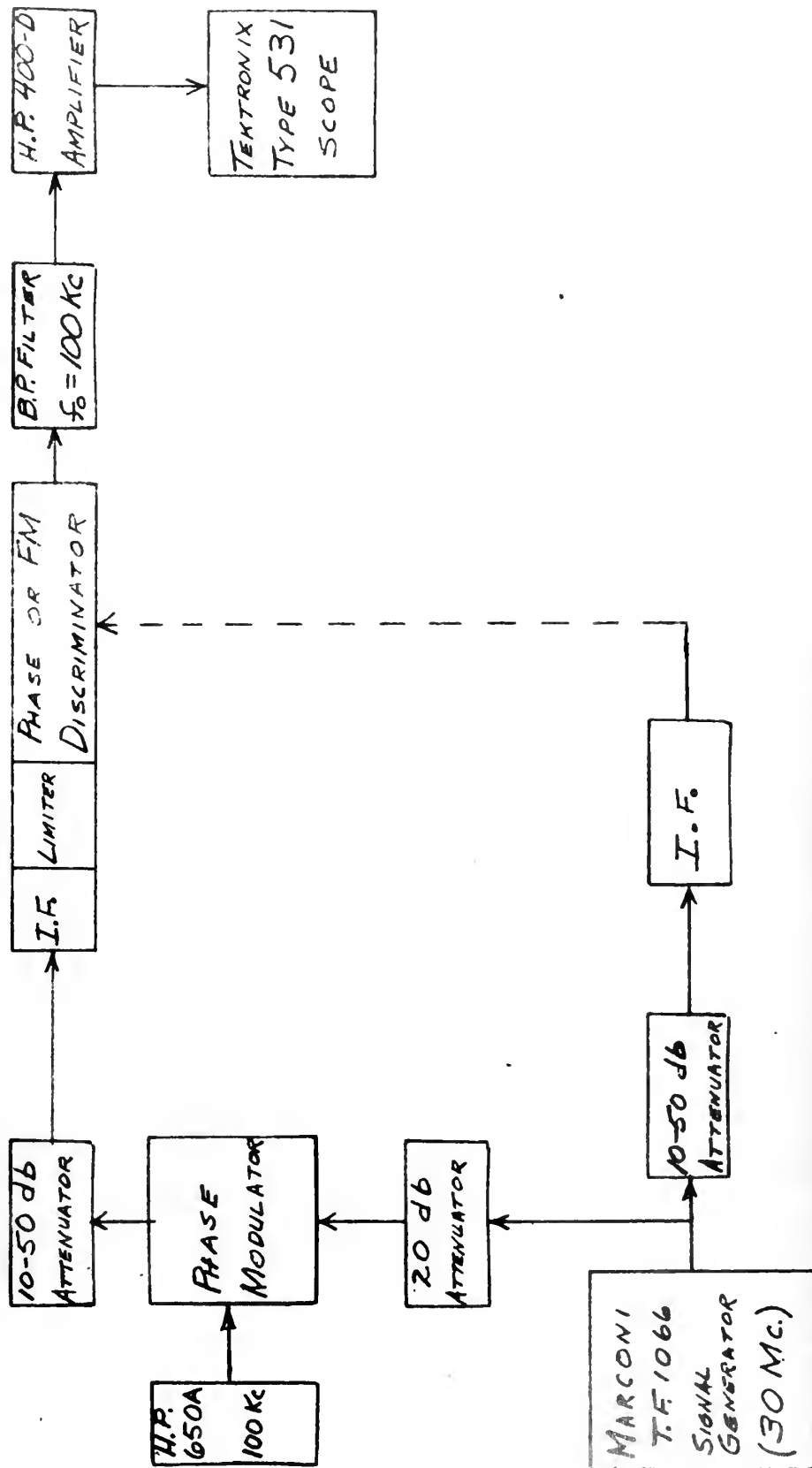


Fig. (6-2)



For each setting of  $S_1$ , the output signal-to-noise ratio ( $S_2$ ) was measured using the two discriminators in succession. All measurements were repeated on different days. Fig. (6-3) shows photographs of the oscilloscope presentations for various levels of  $S_1$ .

Eq. (5-8) may be used to determine  $S_2$ . In order to compare with the laboratory set-up, let

$$\begin{aligned} f_1 &= 100 \text{ Kc} \\ \beta_1 &= .27 \\ B &= 2 \text{ Mc} \\ 2\gamma &= 6.6 \text{ Kc} \end{aligned}$$

where  $2\gamma$  is the effective noise bandwidth of the post detection filter and is calculated from its measured 3 db bandwidth using the table on p. 177 of Threshold Signals. This table also indicates that for the six single-tuned stages of the I.F. amplifier, the noise bandwidth closely approaches the 3 db bandwidth.

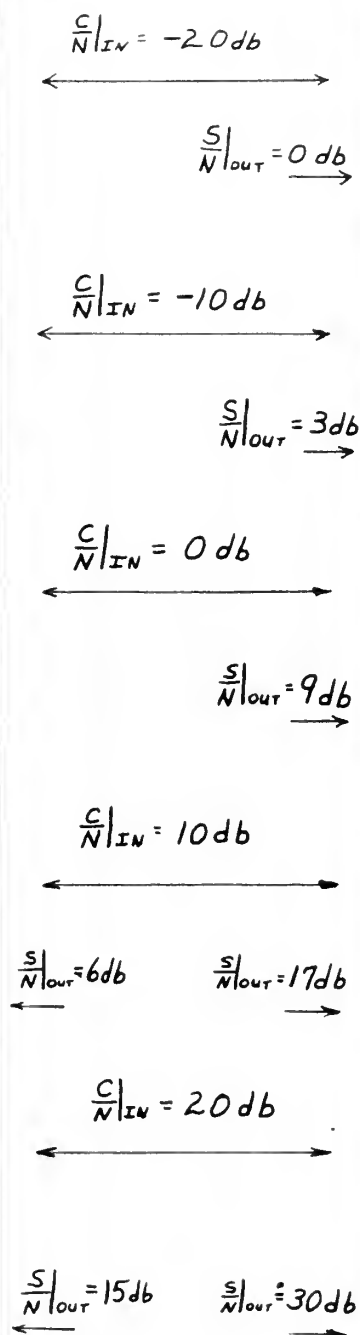
Since  $S_1 = \frac{E_s^2}{2\sigma^2}$  and  $f_1 = .05B$ , Eq. (5-8) may be used to give

$$\begin{aligned} S_2 &= \frac{\text{SIGNAL POWER @ } f_1}{\text{NOISE POWER IN OUTPUT}} \\ &= \frac{\beta_1^2 B S_1}{4\gamma} \cdot \frac{\left\{ 4\left[1 - \frac{1}{R^2}\right]^2 - \frac{2}{S_1 R^2} \left[1 - \frac{1}{R^2}\right] + \frac{1}{4S_1^2 R^4} \right\}}{\left\{ \frac{2\beta_1^2}{R^4} + \frac{.475\beta_1^2}{S_1 R^4} + \frac{1}{S_1} \left[ 4S_1 \left(1 - \frac{1}{R^2}\right)^2 - \frac{2}{R^2} \left(1 - \frac{1}{R^2}\right) + \frac{1}{4S_1^2 R^4} \right] + \frac{3.8}{R^4} + \frac{3}{8S_1^2 R^4} \right\}} \\ &= \frac{11.05 S_1 \left\{ 4\left(1 - \frac{1}{R^2}\right)^2 - \frac{2}{S_1 R^2} \left(1 - \frac{1}{R^2}\right) + \frac{1}{4S_1^2 R^4} \right\}}{\left\{ \frac{.1458}{R^4} + \frac{.0346}{S_1 R^4} + \left[ 4\left(1 - \frac{1}{R^2}\right)^2 - \frac{2}{S_1 R^2} \left(1 - \frac{1}{R^2}\right) + \frac{1}{4S_1^2 R^4} \right] + \frac{3.8}{R^4} + \frac{.375}{S_1^2 R^4} \right\}} \quad (6-1) \end{aligned}$$





FM DISCRIMINATOR



PHASE DISCRIMINATOR,  
COHERENT REFERENCE

$$\beta_{I.F.} = .27 ; f_{mod} = 100\text{Kc} ; f_c = 30\text{Mc.}$$

Fig. (6-3)



Curves of  $S_2$  vs.  $S_1$  for  $R = 10$  and  $R = 5$  are computed from Eq. (6-1) and are shown in Fig. (6-4). If the additional condition is imposed that

$$E_s^2 \ll \langle E_R^2 \rangle \sigma^2,$$

then the asymptotic condition exists wherein

$$S_2 = K S_1, \quad (6-2)$$

where  $K$  depends upon  $\beta_1$ . This curve is also shown in Fig. (6-4).

Fig. (6-5) is a plot of experimental data showing the effect upon  $S_1$  of varying the ratio  $R$ .

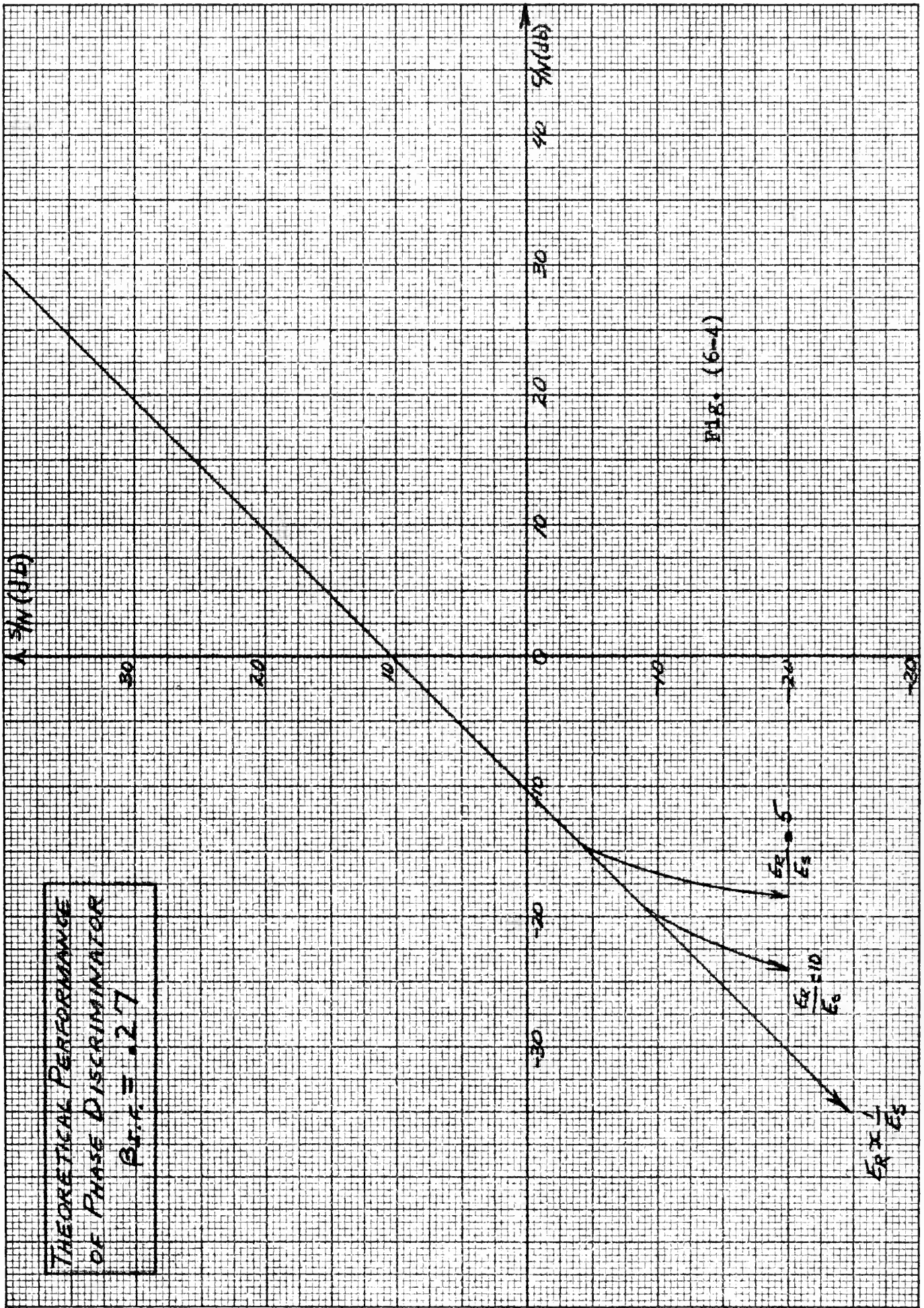
Fig. (6-6) is a comparison between theoretical and experimental results when the conditions of Eq. (6-2) are met.

Fig. (6-7) is a comparison of phase- and frequency-discriminator performance for a smaller modulation index,  $\beta_1 = .125$ . The theoretical result predicted by Eq. (6-2) is also shown.





THEORETICAL PERFORMANCE  
OF PHASE DISCRIMINATOR  
 $B_{\phi} = 2.7$





PHASE DISCRIMINATOR  
PERFORMANCE FOR  
VARIOUS RATIOS OF  
 $E_R/E_S$ . (EXPERIMENTAL)

Δ  $E_R = 10 E_S$   
○  $E_R = 5 E_S$

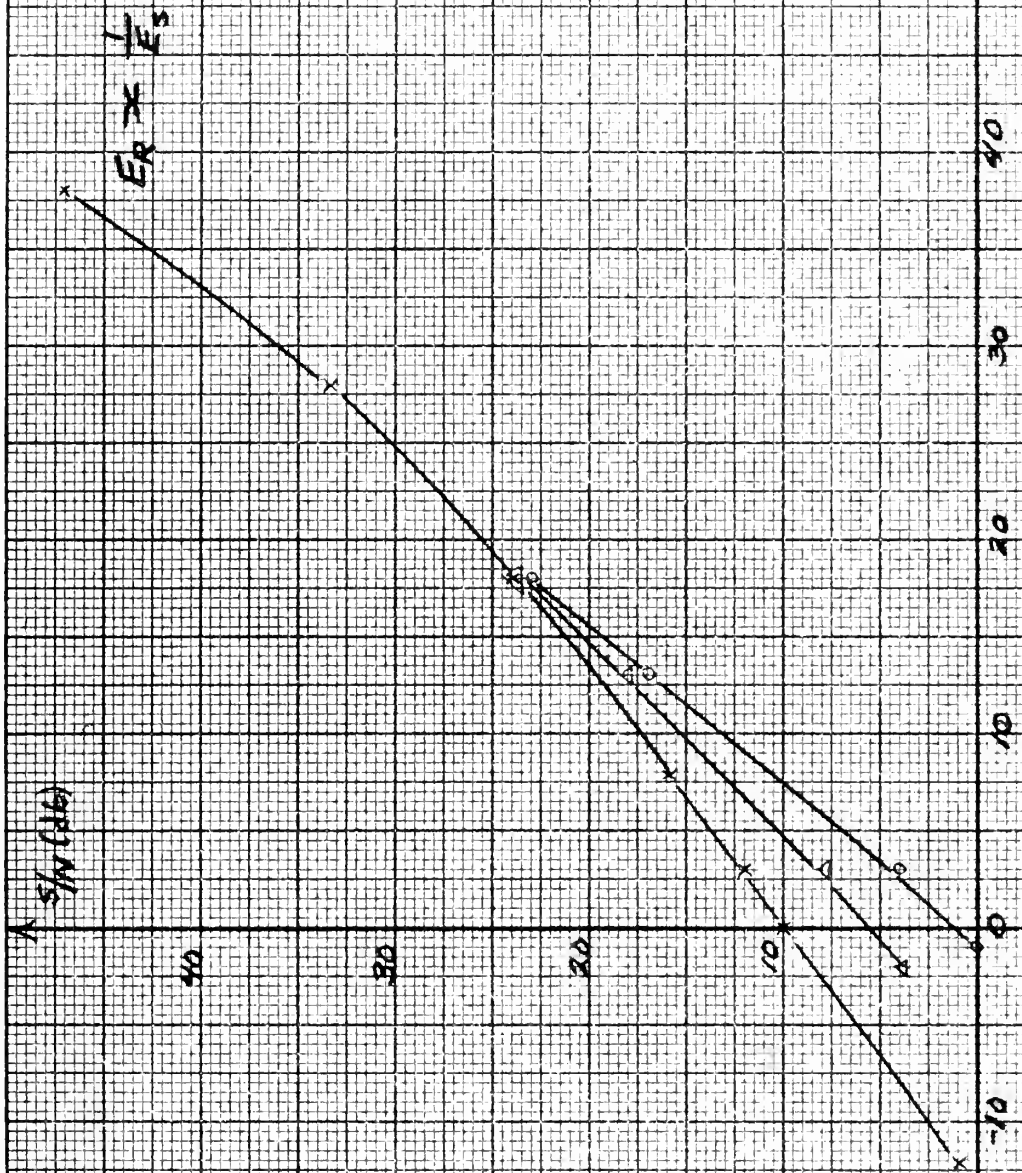
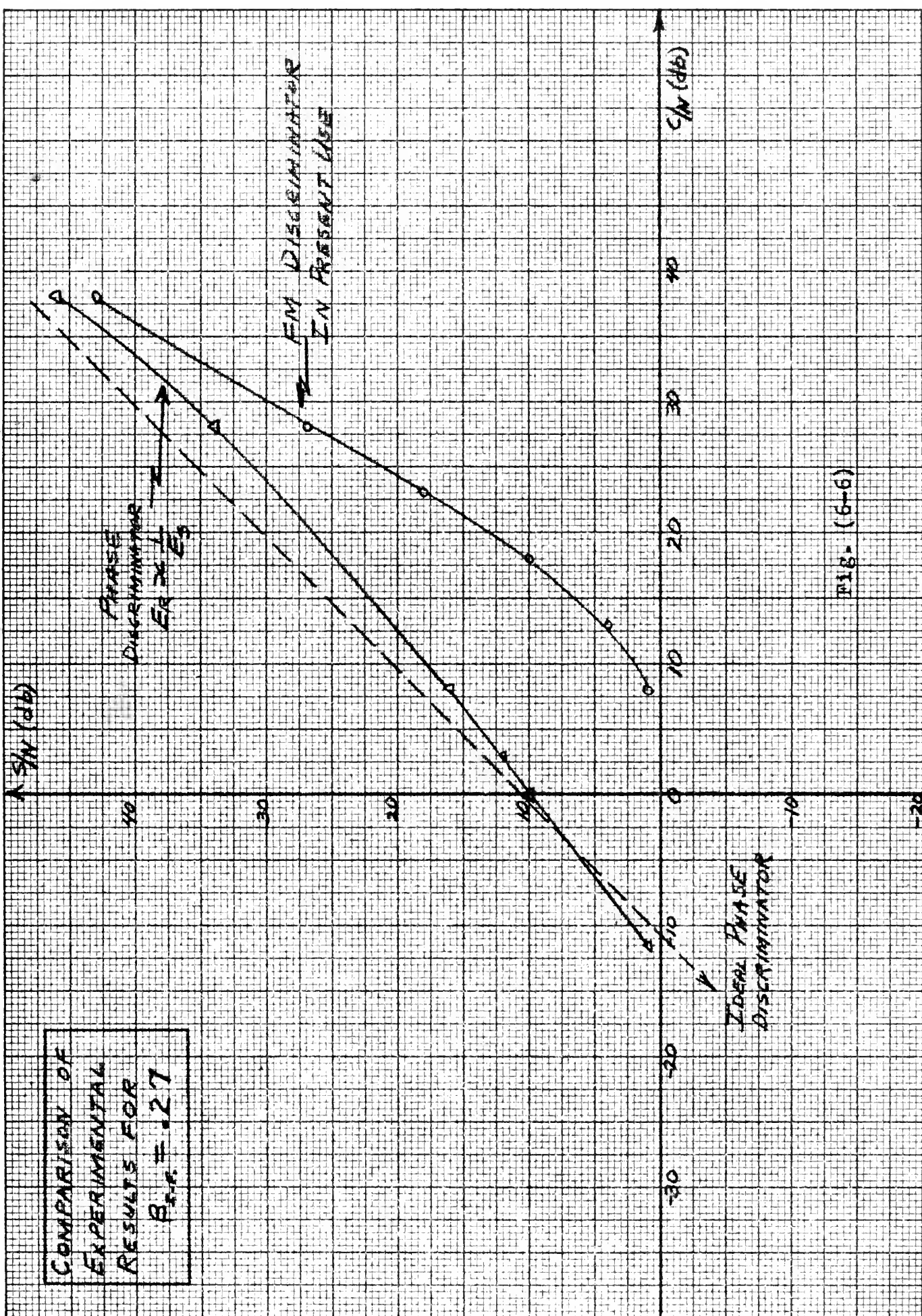


Fig. (6-5)









COMPARISON OF  
EXPERIMENTAL  
RESULTS FOR

$$P_{s.p.} = 0.125$$

SN(dB)

SN(dB)

PHASE DISCRIMINATOR

$$E_R = \frac{1}{E_S}$$

FM DISCRIMINATOR  
IN PRESENT USE

IDEAL PHASE  
DISCRIMINATOR

FIG. (6-7)





## 7. Automatic Gain Control (AGC).

The present transponder circuitry employs a limiter stage and AGC to the first four I.F. stages. The AGC detector is an unbiased crystal diode. Both AGC and limiting are considered necessary because of the large range of input carrier level. The prospect of increasing range even further by using the phase discriminator has aroused interest in an evaluation of different types of AGC.

Of primary interest in this evaluation are the relative effects upon phase shift through the I.F. amplifier and limiter as the carrier level varies over the range. The change in phase shift through these components is attributed to variations in the input capacity with bias voltage. A change in bias voltage alters the gain of the stage (which in turn changes the input capacity due to the Miller effect) and the direct plate current (which changes the grid-cathode impedance due to its effect on the size of the virtual cathode). The present I.F. amplifier is considered sufficiently insensitive to these variations that it can be used with the present AGC or either of two proposed types of AGC. Accordingly, the manner in which limiter operating point varies with the strength and composition of the signal at its grid will be considered.

The input circuit of the limiter stage is shown in Fig. (7-1). If the path from G to ground is regarded as an ideal linear rectifier in series with a fixed resistance  $R_x$ , an equivalent circuit may be drawn as in Fig. (7-2).



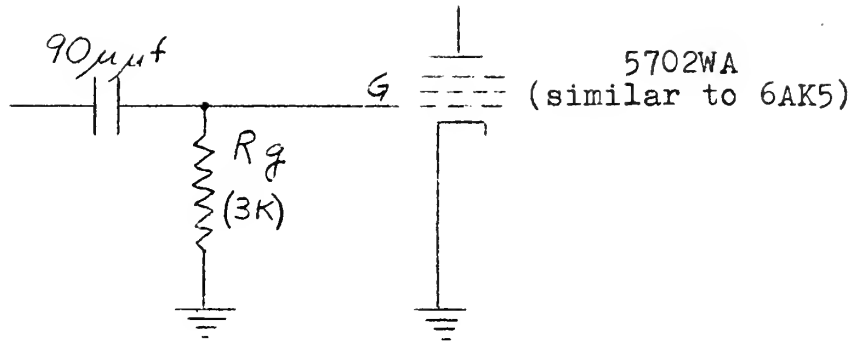


Fig. (7-1)--Limiter input circuit

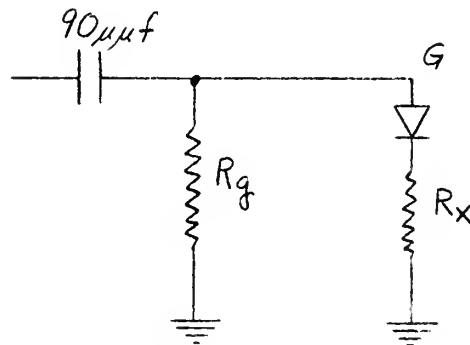


Fig. (7-2)--Equivalent circuit

Since the grid path will conduct in only one direction and the capacitor will pass no direct current, any direct current flowing through the crystal must return to G through the 3K resistor. The d.c. grid bias is thus

$$E_A = R_g I_{x_{d.c.}} \quad (7-1)$$

The presence of  $E_A$  creates a biased linear rectifier. Let the input voltage be

$$S(t) + n(t) = E_s \sin \omega_o t + n(t) \quad (7-2)$$



where the signal portion is considered unmodulated to make calculations more simple. Since the actual signal is frequency-modulated and a time average will be taken to obtain the d.c. component, the result obtained by using Eq. (7-2) will be correct.

The noise voltage is taken to be Gaussian with a first probability distribution

$$W_1 = \frac{1}{\sigma \sqrt{2\pi}} e^{-\frac{n^2}{2\sigma^2}} \quad (7-3)$$

Current flows through the diode when  $S(t) + n(t) - E_A \geq 0$  where  $E_A$  is the d.c. bias voltage. Replacing  $S(t) + n(t) - E_A$  by the random variable  $Z$  and using the relation (9)

$$W_1(Z) = f[Z + E_A - S(t)] \quad (7-4)$$

where  $f(n)$  is the first probability distribution of  $n$ , the first probability distribution of  $Z$  is obtained,

$$W_1(Z) = \frac{1}{\sigma \sqrt{2\pi}} e^{-\frac{[Z + E_A - S(t)]^2}{2\sigma^2}} \quad (7-5)$$

Now  $I_{X_{d.c.}} = \frac{1}{R_x} \overline{[S(t) + n(t) - E_A]}$  where the ensemble average is taken over the region  $S(t) + n(t) - E_A > 0$ , or

$$I_{X_{d.c.}} = \frac{1}{R_x} \overline{Z} \quad (7-6)$$

over all positive  $Z$ . The ensemble average is taken first

$$\overline{Z} = \frac{1}{\sigma \sqrt{2\pi}} \int_0^{\infty} Z e^{-\frac{[Z + E_A - S(t)]^2}{2\sigma^2}} dZ$$



$$\bar{Z} = \frac{1}{\sigma \sqrt{2\pi}} \int_{E_A - S(t)}^{\infty} \mu e^{-\frac{\mu^2}{2\sigma^2}} d\mu + \frac{S(t) - E_A}{\sigma \sqrt{2\pi}} \int_{E_A - S(t)}^{\infty} e^{-\frac{\mu^2}{2\sigma^2}} d\mu.$$

The first integral on the right is integrated directly to give

$$\frac{1}{\sigma \sqrt{2\pi}} \int_{E_A - S(t)}^{\infty} \mu e^{-\frac{\mu^2}{2\sigma^2}} d\mu = \frac{\sigma}{\sqrt{2\pi}} e^{-\frac{[S(t) - E_A]^2}{2\sigma^2}}.$$

Replacing  $\frac{\mu^2}{2\sigma^2}$  by  $t^2$  in the second integral on the right, and using the relation (12)

$$\int_0^{\infty} e^{-t^2} dt = \frac{\sqrt{\pi}}{2}$$

the result is

$$\frac{S(t) - E_A}{\sigma \sqrt{2\pi}} \int_{E_A - S(t)}^{\infty} e^{-\frac{\mu^2}{2\sigma^2}} d\mu = \frac{S(t) - E_A}{2} + \frac{\sqrt{2} [S(t) - E_A]}{\sqrt{2\pi}} \int_0^{\frac{1}{\sigma\sqrt{2}} [S(t) - E_A]} e^{-t^2} dt.$$

Thus,

$$\bar{Z} = \frac{\sigma}{\sqrt{2\pi}} \left\{ e^{-\frac{[S(t) - E_A]^2}{2\sigma^2}} + \left[ \frac{S(t) - E_A}{\sigma} \right] \sqrt{\frac{\pi}{2}} + \frac{\sqrt{2} [S(t) - E_A]}{\sigma} \int_0^{\frac{1}{\sigma\sqrt{2}} [S(t) - E_A]} e^{-t^2} dt \right\} \quad (7-7)$$

From Eq. (7-1) and (7-6) a conditional equation can be written for  $E_A$ .





$$E_A = \left( \frac{R_g}{R_x} \right) \left( \frac{\sigma}{\sqrt{2\pi}} \right) \cdot \left\{ \epsilon^{-\frac{[S(t)-E_A]^2}{2\sigma^2}} + \frac{[S(t)-E_A]}{\sigma} \sqrt{\frac{\pi}{2}} + \frac{\sqrt{2}[S(t)-E_A]}{\sigma} \int_0^{\frac{1}{\sigma\sqrt{2}}[S(t)-E_A]} \epsilon^{-t^2} dt \right\} \quad (7-8)$$

It does not appear that Eq. (7-8) can be expressed in closed form. Bennett (1), on p. 170 of his paper, implied that numerical methods are necessary to solve this problem. However, for a given value of carrier-to-noise ratio, the numerical integration required to determine the time average is not too tedious. Values of  $I_{d.c.}$  for  $-10\text{db} < S_1 < +10\text{db}$  are of primary interest, since Middleton (17) and Rice (19) have written expressions for, respectively, the no-signal case and very large carrier-to-noise ratios. In fact, with  $S(t) = 0$ , Eq. (7-7) reduces to Eq. 4-3, p. 785 of Middleton's paper. It will be shown later that for large  $S_1$ , results obtained from Eq. (7-8) are very nearly the same as those given by Rice on p. 123 of his paper (Vol. 24).

An example will be used to illustrate the method of numerical integration. Starting with Eq. (7-8) and choosing

$$S_1 = \frac{E_s^2}{2\sigma^2} = 1, \text{ the result is}$$

$$E_A = \frac{\sigma R_g}{R_x \sqrt{2\pi}} \left\{ \frac{-E_A}{\sigma} \sqrt{\frac{\pi}{2}} + \epsilon^{-\left(\frac{\sin \omega_c t - \frac{E_A}{\sigma\sqrt{2}}}{\sigma\sqrt{2}}\right)^2} + 2 \left( \frac{\sin \omega_c t - \frac{E_A}{\sigma\sqrt{2}}}{\sigma\sqrt{2}} \right) \int_0^{\frac{\sin \omega_c t - \frac{E_A}{\sigma\sqrt{2}}}{\sigma\sqrt{2}}} \epsilon^{-t^2} dt \right\} \quad (7-9)$$

where use is made of the fact that  $\sin \omega_c t = 0$ .



In the actual circuit  $R_g$  is  $3K\Omega$ . An arbitrary value of  $1K\Omega$  is assigned to  $R_x$ . This will affect the numerical results but not the general conclusions to be reached. A value is now assigned to  $\frac{E_A}{\sigma\sqrt{2}}$  and the two terms to be averaged are plotted on graph paper from  $\omega_0 t = -\frac{\pi}{2}$  to  $+\frac{\pi}{2}$  in steps of 0.2 radians. The average value of each term is computed from the number of squares under the curve and the right side of the equation is thus reduced to a fraction of  $E_A$ . The process is repeated for different values of  $\frac{E_A}{\sigma\sqrt{2}}$  until the right side is just  $E_A$ .

Values for  $E_A$  were computed in this manner for carrier-to-noise ratios of zero, six, and ten decibels. In the tabulation below,  $E_A$  is expressed as a fraction of  $P_t$ , defined by

$$P_t \triangleq \sigma^2 + \frac{E_s^2}{2}, \quad (7-10)$$

and equal to the r.m.s. power which would be dissipated by the input voltage if it were impressed upon a one-ohm resistor:

<u><math>S_1</math>(db)</u>	<u><math>E_A</math></u>
Less than -10	.552 $P_t$
0	.565 $P_t$
6	.600 $P_t$
10	$\left\{ \begin{array}{l} .601 P_t \\ .607 P_t \end{array} \right.$ <span style="display: inline-block; vertical-align: middle; margin-left: 10px;">           (Numerical Integration)            (Rice's Approximation)         </span>

The conditions for Rice's approximation are not fully met, since he required  $E_S - E_A \gg \sigma$  and for  $S_1 = 10\text{db}$ ,  $E_S - E_A = 3\sigma$ .

An inspection of this tabulation reveals that the input voltage may vary from "pure carrier" to "pure noise" with an accompanying variation in limiter self-bias of less than 10



percent, provided that the mean square power input to the limiter is kept constant.

Both of the proposed AGC systems are based upon circuitry which would present an extremely narrow bandwidth to noise. The system in Fig. (1-1) utilizes a crystal oscillator to translate downward in frequency a portion of the I.F. voltage. At this lower frequency ( $100 K_c$ ) the bandwidth may be reduced conveniently to  $15 K_c$ . The carrier-to-noise ratio after the bandwidth reduction ( $S_1'$ ) is then related to  $S_1$  by

$$\frac{2 \times 10^6}{15 \times 10^3} = \frac{S_1'}{S_1}$$

or,

$$S_1' = 133.3 S_1$$

$$S_1'(db) = S_1(db) + 21.2 db.$$

Thus the AGC detector is only slightly affected by noise until the carrier is greatly reduced below noise.

The other system is also a "carrier-only" type. Here the reference voltage  $E_R \cos \omega_c t$  would be shifted in phase by  $90^\circ$  and multiplied by a portion of the I.F. voltage. The output circuit of the multiplier would have a very low cut-off frequency, hence a low equivalent noise bandwidth and the d.c. output would be proportional to the carrier level in the I.F. voltage wave.

The simple diode which acts as the detector in the present AGC system has been investigated quite thoroughly by Rice (19). His Eq. (4.1-14) shows that for a quadratic detector

$$I_{d.c.} = \alpha \left[ \sigma^2 + \frac{E_s^2}{2} \right], \quad (7-11)$$

where  $\alpha = \text{constant}$ .



Using the notation of Eq. (7-10) this may be written

$$I_{d.c.} = \alpha P_t. \quad (7-12)$$

Similarly for a linear rectifier Rice obtained

$$I_{d.c.} = \frac{\alpha \sigma}{\sqrt{2\pi}} e^{-\frac{S_1}{2}} \left[ (1+S_1) I_0\left(\frac{S_1}{2}\right) + S_1 I_1\left(\frac{S_1}{2}\right) \right] \quad (7-13)$$

where  $I_0$  and  $I_1$  are Bessel functions of imaginary argument.

Again using Eq. (7-10) and the relation  $S_1 = \frac{E_s^2}{2\sigma^2}$ , Eq. (7-13) may be written

$$I_{d.c.} = \left( \frac{\alpha \sqrt{P_t}}{\sqrt{2\pi}} \right) \left[ \frac{e^{-\frac{S_1}{2}}}{\sqrt{1+S_1}} \left\{ (1+S_1) I_0\left(\frac{S_1}{2}\right) + S_1 I_1\left(\frac{S_1}{2}\right) \right\} \right]. \quad (7-14)$$

In Appendix C it is shown that the quantity within square brackets is very nearly unity over the entire range of  $S_1$  from 0 to  $\infty$ . Hence, for the linear detector

$$I_{d.c.} \doteq \text{constant} \times \sqrt{P_t}.$$

If ideal AGC action is assumed, it is apparent that the crystal diode detector tends to maintain the total power output from the I.F. amplifier constant. The "carrier-only" AGC tends to keep  $E_s$  constant. From Eq. (7-10), by substituting  $\frac{E_s^2}{2S_1} = \sigma^2$  the result is

$$P_t = \frac{E_s^2}{2} \left( 1 + \frac{1}{S_1} \right). \quad (7-15)$$

For  $S_1 < 1$ , decreasing  $S_1$  requires that  $P_t$  increase at a rate proportional to  $S_1^{-2}$ . Cubic anticipates that eventually the equipment will operate down in the region where  $S_1$  approaches -20db. It is apparent that in a system which has appreciable gain for large carrier-to-noise ratios, the requirement of Eq. (7-15) cannot be met with a practical





amplifier for  $S_1 \ll 1$ . Jaffe and Rechtin (13) have pointed out this inapplicability of "carrier-only" AGC to systems requiring a large dynamic range.

There is another aspect of the AGC problem worthy of consideration. From Eq. (5-8) it is seen that the signal power out of the phase discriminator is proportional to  $\beta_1^2$ . The phase discriminator is followed by a "compensating amplifier" of fixed gain which amplifies the five modulating frequencies before they are used to phase modulate a carrier. This carrier is then multiplied up in frequency until it is 30 Mc below the incoming carrier frequency, a process which also multiplies the modulation index by the same factor (22). The modulation index out of the phase modulator at any given modulating frequency is proportional to the voltage at that frequency (3). Hence, the modulation index of the retransmitted wave depends upon  $E_s \beta_1$ . But

$$\beta_1 = \beta_R - \beta_T \quad (7-16)$$

where  $\beta_R$  = modulation index at  $f_1$  of incoming signal.  
 $\beta_T$  = modulation index at  $f_1$  of retransmitted signal.

Thus, if the circuit employs an AGC system which tends to maintain  $P_t$  constant, a reduction in  $S_1$  will result in a smaller value of  $E_s$ , which in turn tends to make  $\beta_1$  increase. Specifically, in the present system,  $\beta_R \doteq 1$ , and for  $S_1 = 10$ ,  $\beta_1 \doteq .02$ . If the phase modulator is assumed to exhibit a linear relation between modulating voltage and modulation index,  $\beta_T = K_1 E_s \beta_1$ . Then from Eq. (7-16),

$$\beta_1 = \beta_R - K_1 E_s \beta_1 = \frac{1}{1 + K_1 E_s} \quad (7-17)$$



Also, from Eq. (7-16), for the conditions given above

$$\beta_T = \beta_R - \beta_1 = \cancel{R_1} E_S (.02) = .98$$

Thus,  $k_1 = \frac{49}{C}$ , where  $C$  is the value of  $E_S$  corresponding to  $S_1 = 10$ , keeping in mind that  $P_t \doteq$  constant.

Now from Eq. (7-15), solving for  $E_S$

$$E_S = \left( \sqrt{2P_x} \right) \left( \sqrt{\frac{S_1}{S_1+1}} \right) \quad (7-18)$$

and,

$$C = \left( \sqrt{2P_x} \right) \left( \sqrt{\frac{10}{10+1}} \right) = \sqrt{\frac{20}{11}} \cdot \sqrt{P_x}$$

from which

$$\cancel{R_1} = 49 \sqrt{\frac{11}{20P_x}}$$

Substituting this quantity for  $k_1$  and using Eq. (7-18), Eq. (7-17) becomes

$$\beta_1 = \frac{1}{1 + 49 \sqrt{\frac{11}{10}} \cdot \sqrt{\frac{S_1}{S_1+1}}} = \frac{1}{1 + 51.4 \sqrt{\frac{S_1}{S_1+1}}} \quad (7-19)$$

Evaluating Eq. (7-19) for  $S_1 = 1/100$  or -20 decibels,

$$\beta_1 \doteq \frac{1}{1 + 51.4 \sqrt{\frac{1}{100}}} = .163$$

From Eq. (6-1) it is noted that for large  $R$ , increasing  $\beta_1$  from .02 to .163 improves the signal-to-noise ratio  $S_2$  by approximately  $\left( \frac{.163}{.02} \right)^2 = 66.5$  or 18.3 db.

It remains to determine the effect of the I.F. amplifier phase shift characteristic upon the phase of the modulating wave at the output of the discriminator. Disregarding the noise voltage, the wave at the input to the first I.F. stage may be written (12)



$$\begin{aligned}
e_i(t) &= A \sin[\omega_0 t + \beta_1 \sin \omega_1 t] \\
&= A \left\{ J_0(\beta_1) \sin \omega_0 t + \sum_{n=1}^{\infty} J_n(\beta_1) \sin[(\omega_0 + n\omega_1)t] \right. \\
&\quad \left. + \sum_{n=1}^{\infty} (-1)^n J_n(\beta_1) \sin[(\omega_0 - n\omega_1)t] \right\} \quad (7-20)
\end{aligned}$$

The phase shift and amplitude response vs. frequency may be obtained from Eq. (3-8) p. 42 of Terman (22),

$$\left. \begin{aligned}
\Theta &= \tan^{-1} \frac{Q\delta(2+\delta)}{(1+\delta)^2} \\
\frac{|A_f|}{|A_{f_0}|} &= \left| \frac{1}{1 + \delta + jQ\delta \frac{(2+\delta)}{(1+\delta)}} \right|
\end{aligned} \right\} \quad (7-21)$$

where

$$\delta = \frac{f}{f_0} - 1.$$

Then the wave at the output of the I.F. amplifier may be written

$$\begin{aligned}
e_o(t) &= B \left\{ J_0(\beta_1) \sin(\omega_0 t - \Theta) \right. \\
&\quad + \sum_{n=1}^{\infty} b_n J_n(\beta_1) \sin[(\omega_0 + n\omega_1)t - \Theta + \phi_n] \\
&\quad \left. + \sum_{n=1}^{\infty} b'_n (-1)^n J_n(\beta_1) \sin[(\omega_0 - n\omega_1)t - \Theta + \phi'_n] \right\}, \quad (7-22)
\end{aligned}$$



where  $b_n$ ,  $\phi_n$  and  $b'_n$ ,  $\phi'_n$  are the amplitude responses and phase shifts at the frequencies  $f_0 + nf_1$  and  $f_0 - nf_1$ , respectively.

Values of  $J_n(\beta_1)$  are tabulated below for  $\beta_1 = .02$  and  $.163$  and  $n = 0, 1, 2, 3$ . All higher orders are zero through at least the fifth decimal.

$J_n \backslash \beta_1$	.02	.163
$J_0$	.99990	.99337
$J_1$	.01000	.08123
$J_2$	.00005	.00332
$J_3$	.00000	.00001

Values of  $b_n$ ,  $\phi_n$ ,  $b'_n$  and  $\phi'_n$  may be obtained from Eq. (7-21) and are tabulated below.

$n$	0	1	2	3
$b_n$	1	.843	.609	.400
$b'_n$	1	.970	.852	.606
$\phi_n$	0	$57.0^\circ$	$109.0^\circ$	$154.1^\circ$
$\phi'_n$	0	$-60.0^\circ$	$-118.9^\circ$	$-177.3^\circ$

Taking  $\beta_1 = .02$ , it is seen from Eq. (7-22) that only the first order sidebands are significant in representing frequency modulation. A phasor diagram of this situation is shown below in Fig. (7-3).





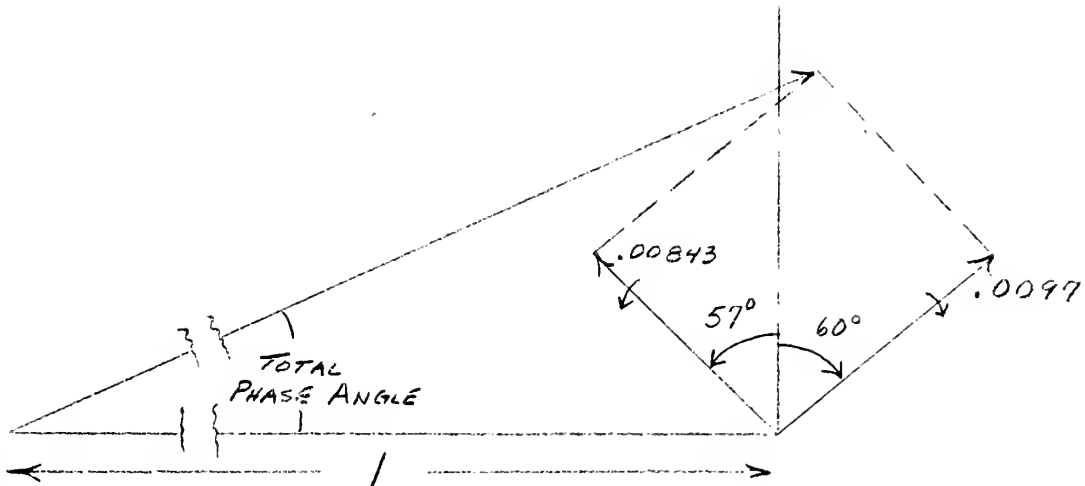


Fig. (7-3)

It can be seen from the diagram and Eq. (7-22) that the phase of the I.F. wave will pass through its zero position when the two first order sidebands are in such a position that their phasor sum has no component perpendicular to the  $\sin \omega_c t$  phasor. This condition is expressed mathematically by writing

$$.843 \sin(1.5^\circ + x) = .97 \sin(1.5^\circ - x), \quad (7-23)$$

from which

$$\sin(1.5^\circ + x) = 1.15 \sin(1.5^\circ - x)$$

$$\sin 1.5^\circ \cos x + \cos 1.5^\circ \sin x = 1.15 \sin 1.5^\circ \cos x - 1.15 \cos 1.5^\circ \sin x$$

$$.15 \sin 1.5^\circ \cos x = 2.15 \cos 1.5^\circ \sin x$$

$$\tan x = \frac{.15}{2.15} \tan 1.5^\circ$$

$$= .00183,$$

$$x \doteq 6.3'. \quad (7-24)$$



This is the amount by which the phase of the wave is shifted from the position it would have if the amplitude response were perfectly symmetrical about  $f_0$ . Even if it were not negligible, it could be calibrated out. It is recorded here simply to illustrate the method of calculation and to serve as a comparison with the phase shifts under different conditions.

Again it is assumed that the I.F. amplifier is correctly tuned to  $f_0$  and  $\beta_1$  is increased to .163. The sidebands at  $f_0 \pm 2f_1$  must now be considered. A phasor diagram of this situation is shown below in Fig. (7-4).

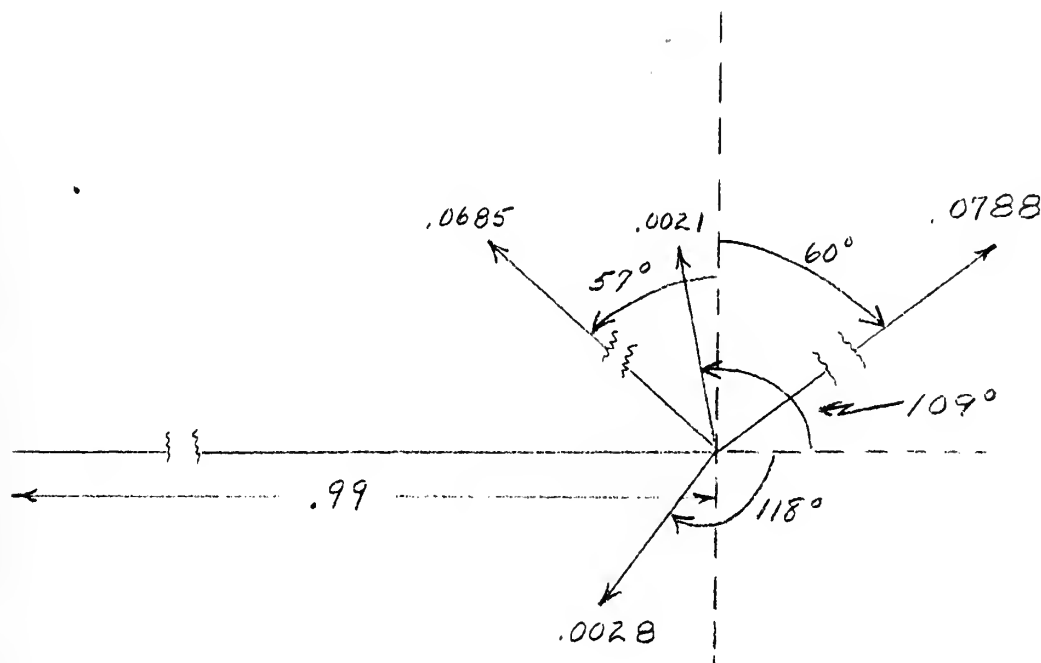


Fig. (7-4)

It appears intuitively that the effective phase shift contributed by the unsymmetrical second order sidebands will be negligible because of their small amplitudes. To show that this is true, assume that the smaller one is removed



completely. The first order sidebands would have a nullifying component perpendicular to the  $\sin \omega_0 t$  reference for a value of  $x$  less than  $10'$  of arc different from that of Eq. (7-24). Since the system accuracy as determined by the servo phasemeter is no better than 1.5 feet and  $10'$  of arc corresponds to approximately 0.92 feet (at the ranging frequency of 491 Kc), the shift in zero axis crossing due to the second order sidebands is obviously negligible.

The above investigation assumed the I.F. amplifier to be correctly tuned to a center frequency  $f_0$ . Now it will be assumed that the carrier frequency remains at  $f_0$  but that the center frequency of the I.F. amplifier is shifted upward to  $f_0 + f_1$ . This is an arbitrary choice but is based upon the fact that the 3db bandwidth is approximately  $4f_1$ , hence a shift in amplifier center frequency of  $f_1$  marks about the maximum shift allowed for in the design "safety factor". The amplifier was of course designed for  $\beta_1 = .02$ , so that only the first pair of sidebands had to be considered.

Taking  $\beta_1 = .02$  and again disregarding the sidebands at  $f_0 \pm 2f_1$ , Eq. (7-22) may be written

$$e_o(t) = B \left\{ .97 J_0(\beta_1) \sin[\omega_0 t - \Theta] \right. \\ \left. + J_1(\beta_1) \sin[(\omega_0 + \omega_1)t - \Theta + 60^\circ] \right. \\ \left. - .852 J_1(\beta_1) \sin[(\omega_0 - \omega_1)t - \Theta - 58.9^\circ] \right\} \quad (7-25)$$



Using the method of Eqs. (7-23) and (7-24) it is found that

$$\chi = -2.6' . \quad (7-26)$$

Now when  $\beta_1 = .163$  it is seen that the amplitudes of the second order sidebands stand in almost exactly the same ratio as in the first case considered, while their phase angles differ by only  $0.3^\circ$ . Thus, the effect upon zero crossings of the second order sidebands is again negligible.

The amplitude modulation which is present when  $\beta_1 = .163$  is at twice the modulating frequency  $f_1$  and is not passed by the tuned circuits of the compensation amplifier.





## 8. Conclusions.

While the analysis of Section 5 is far from rigorous, it is considered a fair conclusion that use of the phase discriminator in place of the frequency discriminator would provide a significant extension of system range. The experimental results of Section 6 support this conclusion. In fact, the experimental results are likely to prove more typical in other discriminators of similar construction, since the assumptions and approximations involved in the work of Section 5 are really quite severe. The assumption that the diodes are perfect switches, for example, is not realistic when the signal is very small. Linear operation of the diodes is similarly unlikely when the signal is very large. Complete symmetry of components is still another condition which is not attainable. However, it is believed that the mathematical model is a reasonable approximation in the region where the r.m.s. reference voltage is maintained very large compared with the total r.m.s. voltage in the I.F. amplifier [conditions of Eq. (6-2)] or carrier-to-noise ratio ( $S_1$ ) is large. This condition is quite easily met when total r.m.s. voltage in the I.F. amplifier is maintained nearly constant. The reference voltage amplitude is simply kept constant at a value which is large with respect to the carrier amplitude where  $S_1 \doteq +10$  db. This is a strong point in favor of using the "constant total power" AGC method of Section 7.

The desirability of keeping circuit changes to a minimum suggests another advantage of retaining the present AGC



system rather than using a "carrier-only" type. Even the addition of an amplifier for the AGC voltage would be relatively simple compared with the extra circuitry required, for example, in Fig. (1-1).



## 9. Recommendations for Further Work.

It appears that the phase discriminator will find many applications in this and other areas of research where phase measurements and/or correlation detection are employed. Radio navigation, radar, color television and many other electronic devices could be cited as examples. Consequently, a really thorough investigation of the phase discriminator might be a highly useful project.

It was mentioned in Section 4 that many non-linear devices have been investigated theoretically to determine their effects on the spectrum of signal plus noise. Regardless of the method used, a fairly common occurrence is the appearance of an integral or infinite series which cannot be expressed in closed form.

Blachman (2), Middleton (17), Rice (19) and Lawson and Uhlenbeck (16) are a few who have reported such results. Their procedure is then to assume "very large carrier-to-noise ratios" and "very small carrier-to-noise ratios" which reduce the equations to closed forms. These results are useful for some practical applications such as the detection of extremely weak signals in noise or circuit response to signal alone. However, equally valid results are often obtainable by the methods of modulation theory for these limiting cases. The region in which calculations are most difficult (carrier-to-noise ratios roughly -20 db to +20 db) would therefore be the region of most practical interest.

It would then seem that a logical approach to a thorough investigation of the phase discriminator problem would involve



a determination of an integral or series form most amenable to solution on a digital computer. Two series might be required to cover the entire range (17) but as long as they could be derived from the initial model without approximations the numerical results could be obtained to any degree of accuracy desired.

Eq. (4-1) requires the knowledge of  $F(j\omega)$  for the device being considered. Rice (19) has tabulated  $F(j\omega)$  for a number of non-linear devices in Appendix 4A of his paper, but no one has written this function for the phase discriminator. This function could probably be calculated with the aid of the papers by Rice (19), Rice and Bennett (20) and Middleton (17). Having obtained this  $F(j\omega)$ , the simplest form for numerical analysis would have to be reasoned out.





## APPENDIX A

### A.1 AVERAGE VALUES

The characteristic function for a random variable  $y$ , or for the corresponding distribution, is defined by (10)

$$\psi(t) = \overline{e^{jty}} = \int_{-\infty}^{\infty} dy W_1(y) e^{jty}. \quad (\text{A.1-1})$$

This result may be generalized for a distribution of  $n$  variables (10) but for the present purpose it is sufficient to write

$$\psi(t_1, t_2) = \int \int_{-\infty}^{\infty} e^{j(t_1 y_1 + t_2 y_2)} W_2(y_1, y_2; \tau) dy_1 dy_2. \quad (\text{A.1-2})$$

Since  $t_1$  and  $t_2$  are constants as far as the integration is concerned, it is possible to differentiate both sides with respect to  $t_1$  and  $t_2$ . Differentiating  $m$  times with  $t_1$  and  $n$  times with  $t_2$  the result is

$$\frac{\partial^{m+n} \psi(t_1, t_2)}{\partial^m t_1 \partial^n t_2} = (j)^{m+n} \int \int_{-\infty}^{\infty} \left\{ y_1^m y_2^n W_2(y_1, y_2; \tau) \exp [j(t_1 y_1 + t_2 y_2)] dy_1 dy_2 \right\}.$$

If now  $t_1$  and  $t_2$  are set equal to zero, the result is

$$\left. \frac{\partial^{m+n} \psi(t_1, t_2)}{\partial^m t_1 \partial^n t_2} \right|_{\substack{t_1=0 \\ t_2=0}} = (j)^{m+n} \int \int_{-\infty}^{\infty} y_1^m y_2^n W_2(y_1, y_2; \tau) dy_1 dy_2.$$



The right side of this equation is just  $(j)^{m+n} \overline{y_1^m y_2^n}$ .

Hence,

$$\overline{y_1^m y_2^n} = (j)^{-m-n} \left[ \frac{\partial^{m+n} \psi(t_1, t_2)}{\partial^m t_1 \partial^n t_2} \right]_{\substack{t_1=0 \\ t_2=0}}. \quad (\text{A.1-3})$$

## A.2 CHARACTERISTIC FUNCTION FOR $W_2$

The characteristic function for  $W_2$  will now be calculated.

$$\begin{aligned} \psi(t_1, t_2) &= \iint_{-\infty}^{\infty} \left\{ \frac{1}{2\pi\sigma^2\sqrt{1-\rho^2}} \exp \left[ j(t_1 y_1 + t_2 y_2) \right] \right. \\ &\quad \cdot \exp \left[ \frac{-1}{2\sigma^2(1-\rho^2)} (y_1^2 + y_2^2 - 2\rho y_1 y_2) \right] dy_1 dy_2 \left. \right\} \\ &= \frac{1}{2\pi\sigma^2\sqrt{1-\rho^2}} \int_{-\infty}^{\infty} \left\{ dy_2 \exp \left[ j t_2 y_2 - \frac{y_2^2}{2\sigma^2(1-\rho^2)} \right] \right. \\ &\quad \cdot \left. \int_{-\infty}^{\infty} dy_1 \exp \left[ j t_1 y_1 - \frac{1}{2\sigma^2(1-\rho^2)} (y_1^2 - 2\rho y_1 y_2) \right] \right\}. \end{aligned}$$

The integration over  $y_1$  is performed first. Completing the square in the exponent the result is

$$\begin{aligned} &\int_{-\infty}^{\infty} dy_1 \exp \left[ j t_1 y_1 - \frac{1}{2\sigma^2(1-\rho^2)} (y_1^2 - 2\rho y_1 y_2 + \rho^2 y_2^2) + \frac{\rho^2 y_2^2}{2\sigma^2(1-\rho^2)} \right] \\ &= e^{\frac{\rho^2 y_2^2}{2\sigma^2(1-\rho^2)}} \int_{-\infty}^{\infty} dy_1 \exp \left[ j t_1 y_1 - \frac{1}{2\sigma^2(1-\rho^2)} (y_1 - \rho y_2)^2 \right]. \end{aligned}$$



Now making the substitution

$$2\pi z = y_1 - \rho y_2$$

this integral reduces to

$$2\pi \cdot \exp\left[\frac{\rho^2 y_2^2}{2\sigma^2(1-\rho^2)} + j t_1 \rho y_2\right] \int_{-\infty}^{\infty} dz \cdot \exp\left[j 2\pi t_1 z - \frac{4\pi^2 z^2}{2\sigma^2(1-\rho^2)}\right]$$

Making use of pair No. 708.0 Campbell and Foster (6) this becomes

$$\sqrt{2\pi\sigma^2(1-\rho^2)} \cdot \exp\left[\frac{\rho^2 y_2^2}{2\sigma^2(1-\rho^2)} + j t_1 \rho y_2 - \frac{t_1^2 \sigma^2(1-\rho^2)}{2}\right]$$

and

$$\begin{aligned} \psi(t_1, t_2) &= \frac{1}{\sqrt{2\pi\sigma^2}} \int_{-\infty}^{\infty} dy_2 \exp\left[j t_2 y_2 - \frac{y_2^2}{2\sigma^2(1-\rho^2)} \right. \\ &\quad \left. + \frac{\rho y_2^2}{2\sigma^2(1-\rho^2)} + j t_1 \rho y_2 - \frac{t_1^2 \sigma^2(1-\rho^2)}{2}\right] \\ &= \frac{e^{-\frac{t_1^2 \sigma^2(1-\rho^2)}{2}}}{\sqrt{2\pi\sigma^2}} \int_{-\infty}^{\infty} dy_2 e^{j y_2 (t_2 + \rho t_1)} e^{-\frac{y_2^2}{2\sigma^2}} \end{aligned}$$

Setting

$$y_2 = 2\pi z$$

and again using pair No. 708.0, this becomes

$$\psi(t_1, t_2) = \frac{\sqrt{2\pi\sigma^2}}{\sqrt{2\pi\sigma^2}} e^{-\frac{t_1^2 \sigma^2(1-\rho^2)}{2}} e^{-\frac{\sigma^2}{2}(t_2 + \rho t_1)^2}$$

which simplifies to

$$\psi(t_1, t_2) = e^{-\frac{\sigma^2}{2}[t_1^2 + 2\rho t_1 t_2 + t_2^2]} \quad (\text{A.2-1})$$



## APPENDIX B

Transformation of Eq. (5-7) requires the determination of the Fourier transforms of  $\cos \omega_1 \tau$ ,  $\rho \cos \omega_1 \tau$ ,  $\rho^2 \cos \omega_1 \tau$ ,  $\rho$ ,  $\rho^2$  and  $\rho^3$ .

As a starting point, it is known that (16)

$$\int_{-\infty}^{\infty} dt e^{-j2\pi ft} = \delta(f) \quad (\text{B-1})$$

where  $\delta(f)$  is the Dirac delta function and has the following properties:

$$\delta(f) = \begin{cases} 0, & f \neq 0 \\ \infty, & f = 0, \end{cases}$$

$$\int_{-\infty}^{\infty} \delta(f) df = 1,$$

$$\delta(f) = \delta(-f)$$

So

$$\int_0^{\infty} \delta(f) df = \frac{1}{2}.$$

To transform  $\cos \omega_1 \tau$ , it is first written

$$\cos \omega_1 \tau = \frac{1}{2} [e^{j\omega_1 \tau} + e^{-j\omega_1 \tau}].$$

So

$$\begin{aligned} \mathcal{F}[\cos \omega_1 \tau] &\triangleq \int_{-\infty}^{\infty} \cos \omega_1 \tau e^{-j\omega \tau} d\tau \\ &= \frac{1}{2} \int_{-\infty}^{\infty} e^{-j2\pi(f-f_1)\tau} d\tau + \frac{1}{2} \int_{-\infty}^{\infty} e^{-j2\pi(f+f_1)\tau} d\tau \end{aligned}$$





$$= \frac{1}{2} \delta(f - f_1) + \frac{1}{2} \delta(f + f_1)$$

or

$$\mathcal{F}[\cos \omega, \tau] = \delta(f - f_1). \quad (\text{positive frequencies}) \quad (\text{B-2})$$

The transform of  $\rho(\tau)$  is obviously

$$\frac{G_N(f)}{\sigma^2} = \begin{cases} 2/B, & 0 < f < B/2 \\ 0, & \text{elsewhere.} \end{cases} \quad (\text{B-3})$$

The transform of  $\rho^2(\tau)$  is most easily taken by using the convolution theorem (25). Thus,

$$\begin{aligned} \int_{-\infty}^{\infty} \rho^2(\tau) e^{-j2\pi f\tau} d\tau &= \frac{1}{\sigma^4} \int_{-\infty}^{\infty} G_N(s) G_N(f-s) ds \\ &= \frac{2}{B} \left[ 1 - \frac{f}{B} \right], \quad 0 < f < B. \end{aligned} \quad (\text{B-4})$$

Denoting the transform of  $\rho^2(\tau)$  by  $H(f)$  and using the convolution theorem again, the transform of  $\rho^3(\tau)$  is found to be

$$\begin{aligned} \int_{-\infty}^{\infty} \rho^2(\tau) \rho(\tau) e^{-j2\pi f\tau} d\tau &= \frac{1}{\sigma^6} \int_{-\infty}^{\infty} H(s) G_N(f-s) ds \\ &= \frac{2}{B^2} \cdot \begin{cases} \frac{3}{4}B - \frac{f^2}{B}, & 0 < f < B/2 \\ \frac{9}{8}B - \frac{3}{2}f + \frac{f^2}{2B}, & B/2 < f < \frac{3}{2}B \\ 0, & \text{elsewhere.} \end{cases} \end{aligned} \quad (\text{B-5})$$



It was seen above (Eq. B-2) that transforming  $\cos \omega_1 \tau$  shifted the spectrum of the unit impulse by  $\pm f_1$ . In an entirely similar manner it is found that

$$\int_{-\infty}^{\infty} \rho \cos \omega_1 \tau e^{-j2\pi f \tau} d\tau = \begin{cases} \frac{2}{B} , & 0 < f < \frac{B}{2} - f_1 \\ \frac{1}{B} , & \frac{B}{2} - f_1 < f < \frac{B}{2} + f_1 \\ 0 , & \text{elsewhere,} \end{cases} \quad (\text{B-6})$$

$$\int_{-\infty}^{\infty} \rho^2 \cos \omega_1 \tau e^{-j2\pi f \tau} d\tau = \begin{cases} 2 - \frac{2f_1}{B} , & 0 < f < f_1 \\ 2 - \frac{2f}{B} , & f_1 < f < B - f_1 \\ 1 - \frac{f - f_1}{B} , & B - f_1 < f < B + f_1 \\ 0 , & \text{elsewhere.} \end{cases} \quad (\text{B-7})$$



# APPENDIX C

Values of  $I_0(x)$  and  $I_1(x)$  for  $0 \leq x \leq 5$  and of  $e^{-x} I_0(x)$  and  $e^{-x} I_1(x)$  for  $6 \leq x \leq 20$  may be obtained from British Association for the Advancement of Science Mathematical Tables, Volume VI. (5).

The expression

$$T(S_1) \stackrel{D}{=} \frac{e^{-\frac{S_1}{2}}}{\sqrt{1+S_1}} \left[ (1+S_1) I_0\left(\frac{S_1}{2}\right) + S_1 I_1\left(\frac{S_1}{2}\right) \right]$$

was evaluated in 3 db increments of  $S_1$  from -15 db to +15 db. Results are tabulated below:

$S_1(\text{db})$	$S_1$	T
-15	.03125	1.000
-12	.0625	1.000
-9	.125	1.000
-6	.25	1.000
-3	.5	1.008
0	1	1.024
3	2	1.045
6	4	1.073
9	8	1.099
12	16	1.110
15	32	1.120

The asymptotic values of  $I_0(x)$  and  $I_1(x)$  are found on p. 271 of the same tables. Substituting these expressions into the right side of the equation for  $T(S_1)$  and letting



$\frac{S_1}{2} = X$ , the result is

$$T(S_1) = \frac{e^{-X}}{\sqrt{1+2X}} \left\{ \frac{(1+2X)e^X}{\sqrt{2\pi X}} \left[ 1 + \frac{1}{8X} + \frac{9}{2(8X)^2} + \dots \right] \right. \\ \left. + \frac{2X e^X}{\sqrt{2\pi X}} \left[ 1 - \frac{3}{8X} - \frac{15}{2(8X)^2} - \dots \right] \right\}.$$

Now letting  $X \rightarrow \infty$  and evaluating the limit,

$$\lim_{S_1 \rightarrow \infty} T(S_1) = \lim_{X \rightarrow \infty} \left\{ \sqrt{\frac{1+2X}{2\pi X}} + \frac{2X}{\sqrt{2\pi X(1+2X)}} \right\} \\ = \lim_{X \rightarrow \infty} \left\{ \sqrt{\frac{\frac{1}{X} + 2}{2\pi}} + \frac{2}{\sqrt{\frac{2\pi}{X} + 4\pi}} \right\} \\ = \left\{ \sqrt{\frac{1}{\pi}} + \sqrt{\frac{1}{\pi}} \right\} \\ = \frac{2}{\sqrt{\pi}} \\ = 1.128.$$

For  $S_1 = 0$ ,

$$T(0) \equiv 1.$$





## BIBLIOGRAPHY

1. Bennett, W. R. "Response of a Linear Rectifier to Signal and Noise", Journal of the Acoustical Society of America, Vol. 15 No. 3, January 1944.
2. Blachman, N. M. "The Demodulation of a Frequency-Modulated Carrier and Random Noise by a Discriminator", Journ. Appl. Physics, Vol. 20 No. 10, October 1949, pp. 976-983.
3. Black, H. S. Modulation Theory, Van Nostrand Company, Inc., New York, 1953.
4. Bode, H. W. Network Analysis and Feedback Amplifier Design, Van Nostrand Company, Inc., New York, 1945.
5. British Association for the Advancement of Science Bessel Functions, Part I, Mathematical Tables, Vol. VI, University Press, Cambridge, 1950.
6. Campbell, G. A. and Foster, R. M. Fourier Integrals for Practical Application, Van Nostrand Company, Inc., New York, 1942.
7. Carson, J. R. "Frequency-Modulation: Theory of the Feedback Receiving Circuit", Bell System Technical Journal, Vol. 18 No. 3, July 1939, pp. 395-403.
8. Chaffee, J. G. "The Application of Negative Feedback to Frequency-Modulation Systems", Bell System Technical Journal, Vol. 18 No. 3, July 1939, pp. 404-437.
9. Cramér, H. The Elements of Probability Theory, John Wiley & Sons, New York, 1955.
10. Cramér, H. Mathematical Methods of Statistics, Princeton University Press, Princeton, 1946.
11. Goldman, S. Information Theory, Prentice-Hall, Inc., New York, 1953.



12. Goldman, S. Frequency Analysis, Modulation and Noise, McGraw-Hill Book Co., Inc., New York, 1948.
13. Jaffe, R.  
and  
Rechtin, E. "Design and Performance of Phase-Lock Circuits Capable of Near-Optimum Performance Over a Wide Range of Input Signal and Noise Levels", I.R.E. Transactions--Information Theory; March 1955.
14. Jensen, G. K.  
and  
McGeogh, J. E. "An Active Filter", NRL Report 4630, Naval Research Laboratory, Washington, D. C., Published by Department of Commerce, Office of Technical Services, 10 November 1955.
15. Knudtson, N. "Experimental Study of Statistical Characteristics of Filtered Random Noise", Res. Lab. of Electronics Tech. Rep't. No. 115, M.I.T. 15 July 1949.
16. Lawson, J. L.  
and  
Uhlenbeck, G. E. Threshold Signals, Rad. Lab. Series, Vol. 24, McGraw Hill Book Company, Inc., New York, 1950.
17. Middleton, D. "The Response of Biased, Saturated Linear and Quadratic Rectifiers to Random Noise", Journ. of Appl. Physics, Vol. 17 No. 10, October 1946.
18. Middleton, D. "Rectification of a Sinusoidally Modulated Carrier in the Presence of Noise", Proc. I.R.E., Vol. 36 No. 12, December 1948, pp. 1467-1477.
19. Rice, S. O. "Mathematical Analysis of Random Noise", Bell System Technical Journal, Vols. 23 and 24, July 1944, January 1945.
20. Rice, S. O.  
and  
Bennett, W. R. "Note on Methods of Computing Modulation Products", Philosophical Magazine, S.7 Vol. 18 No. 119, September 1934.



21. Standards Committee "Standards on Modulation System:  
1952-1953  
A. G. Jensen,  
Chairman  
Definitions of Terms, 1953", Proc.  
I.R.E., Vol. 41 No. 5, May 1953,  
pp. 612-615.
22. Terman, F. E. Radio Engineering, 3d Edition,  
McGraw-Hill Book Company, Inc.,  
New York 1947.
23. Van Voorhis, S.N. Microwave Receivers, Rad. Lab.  
Series, Vol. 23, McGraw Hill Book  
Company, Inc., New York 1948.
24. Wiener, N. "Generalized Harmonic Analysis",  
Acta Mathematica, Vol. 55, 1930,  
pp. 117-258.
25. Woodward, P. M. Probability and Information Theory,  
with Applications to Radar, McGraw  
Hill Book Company, Inc., New York,  
1953.













SE 20 57  
JA 27 60

4735  
5308

Thesis  
S55 Skinner

35727

An analysis of a narrow-  
band frequency modulation  
instrumentation problem.

SE 20 57  
JA 27 60

4735  
5308

Thesis  
S55

Skinner

35727

An analysis of a narrow-band  
frequency modulation instrument-  
ation problem.

thesS55

An analysis of a narrow-band frequency m



3 2768 002 01123 1

DUDLEY KNOX LIBRARY